

Summer 8-4-2021

Finite Element Approximation of Solutions of the Equations of Electroporoelasticity

Yu Hu

Southern Methodist University, huy@smu.edu

Follow this and additional works at: https://scholar.smu.edu/hum_sci_mathematics_etds



Part of the [Partial Differential Equations Commons](#)

Recommended Citation

Hu, Yu, "Finite Element Approximation of Solutions of the Equations of Electroporoelasticity" (2021). *Mathematics Theses and Dissertations*. 17.
https://scholar.smu.edu/hum_sci_mathematics_etds/17

This Dissertation is brought to you for free and open access by the Mathematics at SMU Scholar. It has been accepted for inclusion in Mathematics Theses and Dissertations by an authorized administrator of SMU Scholar. For more information, please visit <http://digitalrepository.smu.edu>.

FINITE ELEMENT APPROXIMATION OF SOLUTIONS
OF THE EQUATIONS OF ELECTROPOROELASTICITY

Approved by:

Dr. Amnon J. Meir
Professor of Mathematics

Dr. Johannes Tausch
Professor of Mathematics

Dr. Thomas Hagstrom
Professor of Mathematics

Dr. Felipe Pereira
Professor of Mathematics

FINITE ELEMENT APPROXIMATION OF SOLUTIONS
OF THE EQUATIONS OF ELECTROPOROELASTICITY

A Dissertation Presented to the Graduate Faculty of the

Dedman College

Southern Methodist University

in

Partial Fulfillment of the Requirements

for the degree of

Doctor of Philosophy

with a

Major in Computational and Applied Mathematics

by

Hu Yu

B.S., Applied Mathematics, China University of Petroleum

M.S., Applied Mathematics, Beijing University of Science and Technology

M.S., Computational and Applied Mathematics, Southern Methodist University

August 4, 2021

Copyright (2021)

Hu Yu

All Rights Reserved

Yu, Hu

B.S., Applied Mathematics, China University of Petroleum
M.S., Applied Mathematics, Beijing University of Science and Technology
M.S., Computational and Applied Mathematics, Southern Methodist University

Finite Element Approximation of Solutions
of the Equations of Electroporoelasticity

Advisor: Dr. Amnon J. Meir

Doctor of Philosophy degree conferred August 4, 2021

Dissertation completed July 27, 2021

In this thesis we consider the solution of the equations of electroporoelasticity, which are a combination of Maxwell's equations and the poroelasticity equations. Included is a description of suitable initial and boundary conditions, weak formulation of the equations, and the error estimate for a general numerical method.

TABLE OF CONTENTS

LIST OF FIGURES	vii
CHAPTER	
1. Introduction	1
1.1. Background	1
1.2. Notations	3
1.2.1. Electromagnetism	3
1.2.2. Poroelasticity	4
1.2.3. Coupling effect	5
1.2.4. Miscellaneous	5
1.3. Function Spaces	5
1.3.1. Differentiable Functions and Distributions	5
1.3.2. Lebesgue and Sobolev Spaces	6
1.3.3. Function Spaces on the Boundary (Trace Spaces) and Related Spaces	7
1.3.4. Basic Spaces involving divergence and curl	7
1.4. Earlier Work	8
1.4.1. General Theory of Three-Dimensional Consolidation	8
1.4.2. Poroelasticity	10
1.4.3. Diffusion in Poroelastic Media	18
1.4.4. Analysis of nonlinear poroelasticity	22
1.4.5. Seismic Phenomena in a Moist Soil	23
1.4.6. Governing equations for the electromagnetics and acoustics	25
1.4.7. Numerical electroseismic modeling: A finite element approach	30
2. Model	36
2.1. Governing Equation	36

2.2. Initial and Boundary Conditions	39
2.3. Weak Form of the Governing Equations	39
2.4. A Priori Estimates	40
2.5. The Operator \mathcal{B}	42
3. Numerical approximation	44
4. Numerical example	57
5. Computation and computer implementation	67

LIST OF FIGURES

Figure	Page
1.1	Types of physical boundary conditions (illustrated in two dimensions): (a) free surface, (b) fluid contact, (c) rigid, frictionless surface, (d) rigid surface in perfect contact (no slippage), (e) infinitely permeable surface, (f) impermeable surface, (g) rigid plate, (h) flexible plate, and (i) bimaterial interface .. 16
4.1	Plot of four variables \mathbf{E} , \mathbf{H} , \mathbf{u} , p 61
4.2	Plot of four variables \mathbf{E} , \mathbf{H} , \mathbf{u} , p 64
4.3	Plot of electromagnetic fields \mathbf{E} and \mathbf{H} 65
4.4	Plot of poroelasticity variables \mathbf{u} and p 66

ACKNOWLEDGMENTS

At the last stage of my PhD program, I'm very grateful for this opportunity, for the colleagues I have met, and for the lessons I have learned.

I would like to express my sincere gratitude to my advisor Prof. Amnon Meir, who pushed me to think bigger and focus on the key questions in my project, and who supported my Ph.D study and research continuously with his his patience and immense knowledge.

I am thankful to the rest of my thesis committee: Prof. Johannes Tausch, Prof. Thomas Hagstrom and Prof. Felipe Pereira, for their insightful questions, comments and encouragement. I am greatly impressed by the brilliant way of showing the existence of solutions of the Maxwell's equations with non-zero electrical conductivity using the Fixed Point Theorem stated by Prof. Hagstrom.

I also would like to thank my family members for supporting me throughout writing this thesis and my life in general, and anyone who has helped me.

This work was partially supported by NSF DMS grant 1619969. The computations were performed on ManeFrame II from the Center for Research Computing, Southern Methodist University.

Chapter 1

Introduction

1.1. Background

“The Earth is a living body. Its soul is its ability to grow. This soul, which also provides the Earth with its bodily warmth, is located in the inner fires of the Earth, which emerge at several places as baths, sulfur mines or volcanoes. Its flesh is the soil, its bones are the strata of rock, its cartilage is the tufa, its blood is the underground streams, the reservoir of blood around its heart is the ocean, the systole and diastole of the blood in the arteries and veins appear on the Earth as the rising and sinking of the oceans.”

—*Leonardo da Vinci (Codex Leicester)*

In Codex Leicester [11], da Vinci drew the analogy between natural objects such as soils, rocks, and tufa to human body tissues like flesh, bones, cartilages and the heart. These materials, from inanimate to organic, have one thing in common, that is, they are all porous materials. Porous materials are solid materials containing void space, or pores, in them. The pores are occupied by fluid, such as water, air, oil, blood, body fluid, or a mixture of fluids.

Poroelasticity is a field in materials science and mechanics that studies porous media. The theory of poroelasticity dates back to Biot’s pioneering work. Biot in a series of papers between 1935 and 1957 [3], [4], [2] developed the general theory of poroelasticity and predicted the propagation of elastic waves. Biot’s equations describe the behavior of fluid-saturated porous media. They are derived from the equations of linear elasticity for the solid matrix, Navier-Stokes equations for the viscous fluid, and Darcy’s law for the flow of fluid through the porous matrix. The theory of poroelasticity has been widely applied in geomechanics, hydrology, biomechanics, tissue mechanics, cell mechanics and micromechanics.

Porothermoelasticity studies the porous media under the influence of heat. It does not assume an isothermal condition. The heat can be, for example, transferred from an adjacent body with different temperature. The resulting deformation itself can generate internal heat, hence the variables in the thermal equations and Biot's equations are coupled. The coupling behavior also applies to chemically active materials in geotechniques, biology, and synthetic material sciences. These materials exhibit swelling or shrinking behaviors when brought in contact with aqueous solutions.

Likewise, the porous media and fluid may interact with electromagnetic fields, then it is then necessary to study the electromagnetic fields and the porous media, and, of course, the interaction between them. The fluid is an electrolyte, thus when the electromagnetic waves propagate through the porous material, the charge excesses at the interface of the solid and the fluid will be acted to produce pressure gradients. If the solid deforms, the resulting relative motions in the fluid will carry excess ions hence generate a current. As a result, the governing equations of electroporoelasticity consist of Maxwell's equations coupled to Biot's equations. Electroporoelasticity arises in many areas from geomechanics [7], [14], [30], [45], to medicine and imaging [22], [28], [29], [31], [32], since both rocks and bones are porous media.

1.2. Notations

We list frequently used notation as follows.

1.2.1. Electromagnetism

We will use ϵ for permittivity and μ for permeability. In sections involving mathematical analysis, ϵ represents infinitesimals as usual. \mathbf{H} , the magnetizing field, is sometimes also known as the magnetic field, so \mathbf{B} is also called flux density or magnetic induction.¹

\mathbf{E}	electric field
\mathbf{B}	magnetic field
\mathbf{H}	magnetizing field
\mathbf{D}	electric displacement
\mathbf{J}_f	ionic-current density
ϵ_0	permittivity of free space
ϵ	permittivity of the material
μ_0	permeability of free space
μ	permeability of the material
σ	electrical conductivity
κ_ξ	dielectric constant
Q	free charge
ω	frequency

¹In [13], the author insists that the name magnetic induction is misleading, since that term already has at least two other meanings in electrodynamics, and \mathbf{B} is indisputably the fundamental quantity. Sommerfeld in [41] also argues that “The unhappy term ‘magnetic field’ for \mathbf{H} should be avoided as far as possible. It seems to us that this term has led into error none less than Maxwell himself ...”.

1.2.2. Poroelasticity

We denote solid or fluid displacement by \mathbf{u} , velocity by \mathbf{v} , relative displacement by \mathbf{w} , and density by ρ .

σ_f	bulk-fluid conductivity
\mathbf{u}_s	solid displacement
\mathbf{u}_f	fluid displacement
$\dot{\mathbf{u}}_s$	instantaneous solid velocity
$\dot{\mathbf{u}}_f$	instantaneous fluid velocity
\mathbf{v}	relative fluid-solid flow vector
\mathbf{w}	relative fluid-solid motion
$\dot{\mathbf{w}}$	filtration velocity
G_{fr}	shear moduli of the framework
p	pressure
ρ_b	bulk density
ρ_s	solid density
ρ_f	fluid density
ϕ	porosity

1.2.3. Coupling effect

The coupling coefficients C , C_{em} , C_{os} depend on the frequency ω .

C bulk-electrolyte molarity

C_{em} electromigration of double layer ions

C_{os} the conductance due to electrically induced streaming of the ions

L frequency dependent coupling coefficient

k permeability

α_∞ tortuosity

1.2.4. Miscellaneous

In mathematical expressions we use caligraphic font for all operators and Mathematical black-bold font for function spaces, to be consistent with \mathbb{R} as it represents the real space.

\mathbf{n} outward normal

$\mathbf{E}, \mathbf{H}, \mathbf{D}$ Math bold font – Vectors

$\mathcal{P}, \mathcal{B}, \mathcal{A}$ Math caligraphy font – Operators

$\mathbb{Q}, \mathbb{V}, \mathbb{R}$ Math black-bold font – Spaces (Custom)

1.3. Function Spaces

We will make use of various functions spaces which we describe below.

In all cases, $\Omega \subset \mathbb{R}^n$ is an open set, $\bar{\Omega}$ its closure and Γ its boundary. Let $\alpha = (\alpha_1, \dots, \alpha_n) \in \mathbb{N}^n$ be a multi-index, with $|\alpha| = \sum_{j=1}^n \alpha_j$.

1.3.1. Differentiable Functions and Distributions

The space $C(\Omega)$ is comprised of all continuous functions on Ω .

$$C(\Omega) = \{f \text{ continuous on } \Omega\}.$$

The space $C^m(\Omega)$ denotes the space of all continuous functions on Ω with continuous derivative up to m -th order.

$$C^m(\Omega) = \{f \in C(\Omega) : \forall \alpha \in \mathbb{N}^n, |\alpha| \leq m, \partial^\alpha f \in C(\Omega)\}, \quad m \in \mathbb{N}.$$

The set of all infinitely differentiable functions on Ω forms the space $C^\infty(\Omega)$.

$$C^\infty(\Omega) = \bigcap_{m \in \mathbb{N}} C^m(\Omega).$$

The space $\mathcal{D}(\Omega)$ comprises of infinitely differentiable functions with compact support on Ω . It is also denoted by C_c^∞ , where the index c stands for compact support.

$$\mathcal{D}(\Omega) = \{f \in C^\infty(\Omega) : f \text{ has compact support in } \Omega\}.$$

A linear and continuous form T defined on $\mathcal{D}(\Omega)$ is called a distribution. The space of distributions is denoted by $\mathcal{D}'(\Omega)$.

$$\mathcal{D}'(\Omega) \text{ is the linear dual of } \mathcal{D}(\Omega) \quad (\text{distributions}).$$

1.3.2. Lebesgue and Sobolev Spaces

The space $L^p(\Omega)$, $1 \leq p < \infty$ is composed of all Lebesgue measurable functions f that are p -integrable, that is, f is defined on Ω such that the integral over Ω of p -th power of f is finite.

$$L^p(\Omega) = \left\{ f \text{ measurable on } \Omega : \int_{\Omega} |f|^p dx < \infty \right\}, \quad 1 \leq p < \infty.$$

The space L^p is endowed with the norm $\|\cdot\|_{L^p(\Omega)}$, $L^p(\Omega)$ is a Banach space and is separable.

The space $L^\infty(\Omega)$ is composed of all Lebesgue measurable functions that are essentially bounded on Ω .

$$L^\infty(\Omega) = \{f \text{ measurable and bounded a.e. on } \Omega\}.$$

A function in the space $H^s(\Omega)$ has square integrable derivatives up to order s . The norm is

$$\text{defined by } \|f\|_{H^s(\Omega)} = \left(\int_{\Omega} \sum_{|\alpha| \leq s} |\partial^\alpha f|^2 dx \right)^{1/2}.$$

$$H^s(\Omega) = \left\{ f \in L^2(\Omega) : \left(\int_{\Omega} \sum_{|\alpha| \leq s} |\partial^\alpha f|^2 dx \right)^{1/2} < \infty \right\}.$$

We define $W^{s,p}(\Omega)$ to be the space of functions f whose derivatives of order less than or equal to s belong to $L^p(\Omega)$, with the norm $\|f\|_{W^{s,p}(\Omega)} = \left(\int_{\Omega} \sum_{j=0}^s |\partial^j f|^p dx \right)^{1/p}$.

$$W^{s,p}(\Omega) = \{f \in L^p(\Omega) : \forall \alpha \in \mathbb{N}^n, |\alpha| \leq s, \partial^\alpha f \in L^p(\Omega)\}, \quad 1 \leq p \leq \infty, s \in \mathbb{N}.$$

The space $W^{s,p}(\Omega)$ is a generalization of $H^s(\Omega)$.

$$H^s(\Omega) = W^{s,2}(\Omega).$$

We further make use of analogous spaces of vector value functions. $\mathbf{L}^2(\Omega) = [L^2(\Omega)]^3$, $\mathbf{H}^1(\Omega) = [H^1(\Omega)]^3$ bold letters denote spaces of multi-dimensional vector fields.

1.3.3. Function Spaces on the Boundary (Trace Spaces) and Related Spaces

Here, Γ is assumed to be a Lipschitz submanifold of \mathbb{R}^n . We denote $\gamma_0 : V \rightarrow W, \gamma_0 f \mapsto f|_{\Gamma}$ the trace mapping on the boundary.

The set of functions of $L^2(\Gamma)$ which are traces of functions of $H^1(\Omega)$ constitutes a subspace of $L^2(\Gamma)$ denoted by $H^{1/2}(\Gamma)$. The dual space of $H^{1/2}(\Gamma)$ is $H^{-1/2}(\Gamma)$ with respect to the $L^2(\Gamma)$ duality pairing.

$$H^{1/2}(\Gamma) = \gamma_0(H^1(\Omega)).$$

$$H^{-1/2}(\Gamma) \text{ is the dual of } H^{1/2}(\Gamma).$$

1.3.4. Basic Spaces involving divergence and curl

The spaces $\mathbf{H}(\mathbf{curl}, \Omega)$ and $\mathbf{H}(\mathbf{div}, \Omega)$ are essential when studying Maxwell's equations or equations of continuum mechanics.

We use $\mathbf{H}(\mathbf{curl}, \Omega)$ to denote the space functions \mathbf{v} which are square integrable, as well as their curl,

$$\mathbf{H}(\mathbf{curl}, \Omega) = \{\mathbf{v} \in \mathbf{L}^2(\Omega) : \mathbf{curl} \mathbf{v} \in \mathbf{L}^2(\Omega)\}.$$

Similarly, the space $\mathbf{H}(\mathbf{div}, \Omega)$ contains all functions in $\mathbf{L}^2(\Omega)$ whose divergence is square integrable,

$$\mathbf{H}(\mathbf{div}, \Omega) = \{\mathbf{v} \in \mathbf{L}^2(\Omega) : \mathbf{div} \mathbf{v} \in L^2(\Omega)\}.$$

The space $\mathbf{H}_0(\mathbf{curl}, \Omega)$ is a subspace of $\mathbf{H}(\mathbf{curl}, \Omega)$. A function in $\mathbf{H}_0(\mathbf{curl}, \Omega)$ has zero tangential components on the boundary, and the integration by parts formula becomes $(\nabla \times \mathbf{u}, \mathbf{v}) = (\mathbf{u}, \nabla \times \mathbf{v})$, where (\cdot, \cdot) is the L^2 inner product,

$\mathbf{H}_0(\mathbf{curl}, \Omega)$ is the closure of $\mathbf{D}(\Omega)$ in $\mathbf{H}(\mathbf{curl}, \Omega)$,

$$\mathbf{H}_0(\mathbf{curl}, \Omega) = \{\mathbf{v} \in \mathbf{H}(\mathbf{curl}, \Omega) : \mathbf{v} \times \mathbf{n}|_{\Gamma} = 0\}.$$

The space $\mathbf{H}_0(\mathbf{div}, \Omega)$ is a subspace of $\mathbf{H}(\mathbf{div}, \Omega)$. A function in $\mathbf{H}_0(\mathbf{div}, \Omega)$ has zero normal components on the boundary, and the integration by parts formula becomes $(\nabla \cdot \mathbf{u}, \mathbf{v}) = -(\mathbf{u}, \nabla \cdot \mathbf{v})$,

$\mathbf{H}_0(\mathbf{div}, \Omega)$ is the closure of $\mathbf{D}(\Omega)$ in $\mathbf{H}(\mathbf{div}, \Omega)$,

$$\mathbf{H}_0(\mathbf{div}, \Omega) = \{\mathbf{v} \in \mathbf{H}(\mathbf{div}, \Omega) : \mathbf{v} \cdot \mathbf{n}|_{\Gamma} = 0\}.$$

The space $\mathbf{H}(\mathbf{curl} 0, \Omega)$ contains functions in $\mathbf{H}(\mathbf{curl}, \Omega)$ that are irrotational, its intersection with $\mathbf{H}_0(\mathbf{curl}, \Omega)$ is written as $\mathbf{H}_0(\mathbf{curl} 0, \Omega)$

$$\mathbf{H}(\mathbf{curl} 0, \Omega) = \{\mathbf{v} \in \mathbf{H}(\mathbf{curl}, \Omega) : \nabla \times \mathbf{v} = 0\}.$$

$$\mathbf{H}_0(\mathbf{curl} 0, \Omega) = \mathbf{H}(\mathbf{curl} 0, \Omega) \cap \mathbf{H}_0(\mathbf{curl}, \Omega).$$

The space $\mathbf{H}(\mathbf{div} 0, \Omega)$ contains functions in $\mathbf{H}(\mathbf{div}, \Omega)$ that are solenoidal, its intersection with $\mathbf{H}_0(\mathbf{div}, \Omega)$ is written as $\mathbf{H}_0(\mathbf{div} 0, \Omega)$

$$\mathbf{H}(\mathbf{div} 0, \Omega) = \{\mathbf{v} \in \mathbf{H}(\mathbf{div}, \Omega) : \nabla \cdot \mathbf{v} = 0\}.$$

$$\mathbf{H}_0(\mathbf{div} 0, \Omega) = \mathbf{H}(\mathbf{div} 0, \Omega) \cap \mathbf{H}_0(\mathbf{div}, \Omega).$$

1.4. Earlier Work

1.4.1. General Theory of Three-Dimensional Consolidation

Maurice A. Biot, is generally recognized as the “father of poroelasticity”. He was awarded the Timoshenko Medal [5], [9]. In [3], he gave a rigorous and complete treatment of consolidation theory. His model describes three-dimensional cases and is valid for arbitrary load which can vary in time.

Soil consolidation is the process that a soil under load will settle gradually with a varying pace, not immediately being crushed. The adaptation of the soil to the load variation is gradual. This phenomenon was first investigated by Terzaghi, except that his treatment was restricted to a one-dimensional problem with constant load. When Biot was generalizing Terzaghi's theory, he adopted Terzaghi's assumptions that the stress-strain relations is revertible under final equilibrium conditions and that the stress-strain relations are linear.

Biot first defined soil stress and explained the relationships between strain, stress, and water pressure, he also interpreted the physical meanings of the coefficients, such as the final compressibility a

$$a = \frac{1 - 2\nu}{2G(1 - \nu)},$$

and the shear modulus G

$$G = \frac{E}{2(1 + \nu)},$$

where ν is the drained Poisson ratio and E is the Young's modulus. We are still using the same definition today.

Biot established the general equations that govern consolidation. They are

$$G\nabla^2 u_1 + \frac{G}{1 - 2\nu} \frac{\partial \nabla \cdot \mathbf{u}}{\partial x} - \alpha \frac{\partial p}{\partial x} = 0, \quad (1.1)$$

$$G\nabla^2 u_2 + \frac{G}{1 - 2\nu} \frac{\partial \nabla \cdot \mathbf{u}}{\partial y} - \alpha \frac{\partial p}{\partial y} = 0, \quad (1.2)$$

$$G\nabla^2 u_3 + \frac{G}{1 - 2\nu} \frac{\partial \nabla \cdot \mathbf{u}}{\partial z} - \alpha \frac{\partial p}{\partial z} = 0, \quad (1.3)$$

$$\kappa \nabla^2 p = \alpha \frac{\partial \nabla \cdot \mathbf{u}}{\partial t} + \frac{1}{Q} \frac{\partial p}{\partial t} \quad (1.4)$$

where $\mathbf{u} = (u_1, u_2, u_3)$ is the solid displacement, p is the fluid pressure, and the final compressibility a and the shear modulus G are defined above. If we write the first three equations as a vector equation, we can see that these equations are the same as (1.15) – (1.16).

Biot then verified his model by doing a standard soil test, he also considered a special case when the porous medium is a saturated clay.

1.4.2. Poroelasticity

Cheng's book [9] is a complete and authoritative reference for poroelasticity, mostly from an engineering and geoscience perspective. The author begins by explaining basic concepts such as drained and undrained responses, time and length scale, and effective stress and poroelastic phenomena like borehole failure and hydraulic fracturing. He lays out a continuum theory of poroelasticity, in terms of bulk constitutive equations, and determines bulk material constants. The main equation is

$$\sigma_{ij} = \left(K_u - \frac{2G}{3} \right) \delta_{ij}e + 2Ge_{ij}, \quad (1.5)$$

where σ is the stress and e is the strain, K_u is the undrained bulk modulus and G the shear modulus.

Then, the author discusses how equations and constants change according to different cases. Many special and ideal models are considered, which provide additional insight into multiple mechanisms.

The spatial averaging method is the applied, thermodynamic principles are explained and variational formulation, and constitutive equations are given, using variation energy minimization principle. A set of intrinsic material constants is determined in the process and the relationship between micromechanical constants is revealed. Laboratory experiments are included.

Next, the author focuses on anisotropy. The general form of constitutive equations and bulk and micromechanical constants are presented. The introduction of different kinds of symmetry has reduced the form of those equations. Orthotropy and transverse isotropy, for example, are both of engineering importance.

The governing equations are summarized, for the linear, isotropic poroelasticity: Definition of strain (a symmetric part of the displacement gradient removes the effect of rotation in the state of strain in a body)

$$e_{ij} = \frac{1}{2} \left(\frac{\partial u_i}{\partial x_j} + \frac{\partial u_j}{\partial x_i} \right).$$

Constitutive equations (stress-strain relations).

$$\tau_{ij} = 2Ge_{ij} + \frac{2G\nu}{1-2\nu}\delta_{ij}e - \alpha\delta_{ij}p$$

$$p = M(\zeta - \alpha e).$$

Equilibrium equation (Newton's law of motion)

$$\frac{\tau_{ij}}{\partial x_j} = 0.$$

Darcy's law (flow of a fluid with constant viscosity across a rock is a function of its pressure difference, and the rock properties)

$$q_i = -\kappa \frac{\partial p}{\partial x_i},$$

Continuity equation (conservation of mass)

$$\frac{\zeta}{\partial t} + \frac{\partial q_i}{\partial x_i} = 0,$$

where ζ is variation in fluid content which is positive for fluid entering the control volume, and q_i is the apparent fluid flux with respect to a nondeformable control volume.

The above equations have a total of twenty variables and a set of five material constants.

The equations can be simplified to obtain the Navier-Cauchy Equation

$$G\Delta\mathbf{u} + \frac{G}{1-2\nu}\nabla(\nabla\cdot\mathbf{u}) = \alpha\nabla p,$$

and the Diffusion Equation

$$\frac{\partial p}{\partial t} - \kappa M\nabla^2 p = -\alpha M \frac{\partial \nabla\mathbf{u}}{\partial t}.$$

These two equations are commonly referred to as the equations of poroelasticity. Simplification of the equations under the assumptions of orthotropy, transverse isotropy, and others that make the equations uncoupled are also included.

Analytical solutions are derived in the next chapter for cases which allow the analytical solutions to be found. Cheng has investigated lower dimensional problems such as a one

dimensional consolidation problem and plane and generalized plane strain, symmetrical cases such as ones with spherical symmetry and axial symmetry, cavity problems, borehole problems, different spatial settings such as a half plane, half space, and cylinder, layered and more.

A long chapter on fundamental solutions and integral equations follows the chapter of analytical solutions. It starts with Green's identities and reciprocity theorems. For fundamental solutions are based on using these identities and theorems. It also explains stress discontinuity method, displacement discontinuity method, dislocation method. Then fundamental solutions for elasticity and poroelasticity are introduced. There is a detailed discussion of the solutions of fluid and solid equations. Topics such as fluid source, fluid dipole, fluid dilatation, solid quadrupole and hexapole, solid center of dilatation, and many more, are studied.

The fully time dependent (dynamic) case - poroelastodynamics - is governed by

$$G\nabla^2\mathbf{u} + (\lambda_u + G)\nabla(\nabla \cdot \mathbf{u}) + \alpha M\nabla(\nabla \cdot \mathbf{w}) = \rho\ddot{\mathbf{u}} + \rho_f\ddot{\mathbf{w}} - \mathbf{F} + \alpha M\nabla Q \quad (1.6)$$

$$\alpha M\nabla(\nabla \cdot \mathbf{u}) + M\nabla(\nabla \cdot \mathbf{w}) - \frac{1}{\kappa}\dot{\mathbf{w}} = \rho_f\ddot{\mathbf{u}} + \rho'\ddot{\mathbf{w}} - \mathbf{f} + M\nabla Q \quad (1.7)$$

where $\mathbf{w} = \phi(\mathbf{u} - \mathbf{v})$ is the specific relative fluid to solid displacement, \mathbf{F} and \mathbf{f} are body forces, and Q is the volume of injected fluid, $\lambda_u = \lambda + \alpha^2 M$ is the undrained Lamé constant, M is the Biot modulus, G , α , ρ and ρ_f are, as usual, the shear modulus, Biot effective stress coefficient, bulk density, and fluid density. Wave propagation phenomenon will occur, due to the existence of the second order time derivative terms. The book includes analytic solutions of some special cases such as one-dimensional and plane wave reflection. It also includes fundamental solutions and singular integral equation representations.

Equations of poroelasticity coupled with equations from other disciplines are always intriguing. Cheng in his book, discusses three cases: poroviscoelasticity, porothermoelasticity and porochemoelasticity. Where poroviscoelasticity is introduced for better describing intergranular frictional sliding, the intrinsic solid grain creep deformation, and more that have

a time scale much smaller than Darcy flow, has apparent viscoelastic mechanisms, and can result in a variety of time-dependent phenomena. Porothermoelasticity deals with the case when the temperature of a porous medium can change, either because the porous medium is in contact with a body of different temperature and heat is transferred by conduction, or because of the heat is generated by deformation itself, and it can not be overlooked. Since there are many types of energy and forces in the physical world, such as electrical, magnetic, and chemical, and their coupling. Porochemoelasticity, is presented to depict the thermochemical influence on the porous media, as many biological and synthetic porous media are chemically active.

It turns out that the effects of thermal energy and chemical substances are identical — the resulting coupled equations have the same form. Analytical solutions in those cases are provided.

The governing equations are listed here for drawing the analogy between equations of porothermoelasticity and porochemoelasticity:

Porothermoelasticity

. Navier Equation

$$G\nabla^2\mathbf{u} + \left(K + \frac{G}{3}\right)\nabla(\nabla \cdot \mathbf{u}) - \alpha\nabla p - \alpha_d\nabla T = 0. \quad (1.8)$$

Note that the pressure p in this equation can be replaced by the fluid content ζ , and the temperature T can be replaced by entropy density s .

. Fluid Diffusion Equation

$$\frac{\partial p}{\partial t} - \kappa M \nabla^2 p = -\alpha M \frac{\partial e}{\partial t} + \beta_e M \frac{\partial T}{\partial t}. \quad (1.9)$$

. Thermal Diffusion Equation

$$\frac{\partial T}{\partial t} - \kappa_T \nabla^2 T = -\frac{\alpha_d}{m_d} \frac{\partial e}{\partial t} + \frac{\beta_e}{m_d} \frac{\partial p}{\partial t} \quad (1.10)$$

Porochemoelasticity

The governing equations consist of

. Navier Equation

$$G\nabla^2\mathbf{u} + \left(K_c + \frac{G}{3}\right)\nabla(\nabla\cdot\mathbf{u}) - \alpha_c\nabla p - \alpha_\mu\nabla c_s = 0. \quad (1.11)$$

Note that the molar concentration c_s can be replaced by osmotic pressure Π , the pressure p , again, can be replaced by the fluid content ζ .

. Diffusion Equations

$$\frac{\partial p}{\partial t} - M_c\kappa_p\nabla^2 p = -M_c\alpha'_c\frac{\partial e}{\partial t} - M_c\beta_\alpha\frac{\partial c_s}{\partial t}, \quad (1.12)$$

$$\frac{\partial c_s}{\partial t} - D'_c\nabla^2 c_s = -\frac{\alpha'_c}{\beta_\beta}\frac{\partial e}{\partial t} - \frac{1}{M_c\beta_\beta}\frac{\partial p}{\partial t}. \quad (1.13)$$

Cheng's discussion of boundary conditions is of special interest to us, since Pride defines the boundary conditions on the shear plane so that boundary conditions he suggests are not practical for computation [34]. We list those boundary conditions here, in the figures.

a) **Free surface.** The surface of the porous medium is not in contact with any medium other than air. The surface traction and pore pressure are zero.

b) **Fluid contact.** The contact surface is a static fluid under pressure $p = p_0$. The normal stress and the pore pressure are the same as the surrounding fluid whose pressure is p_0 and there is no shear stress.

c, d) **Rigid surface smooth or rough.** The surface of the porous medium is in contact with another much harder medium, the contacted surface is considered *rigid*. On a rigid surface, we can either assume a frictionless contact which allows lateral movement (c), or a perfect contact such that no lateral displacement can occur (d).

e, f) **Permeable and impermeable surface.** The permeability of the contact surface is much larger than that of the porous medium. We can assume infinite permeability, so that the pores are drained and pressure is zero (e). Or if instead the permeability is much

smaller, we can assume an impermeable surface, which means that the normal flux is zero (f).

g) **Rigid plate.** A force is applied to a porous medium through a rigid or flexible plate. For a rigid plate, we only know that the displacement on the contacting surface must conform to the rigid shape of the plate. In addition

$$\int_A t_y d\mathbf{x} = \mathbf{F} \quad (1.14)$$

where \mathbf{F} is the applied force, A is the area of the plate. The boundary condition for Darcy's equation can be drained or impermeable.

h) **Flexible plate.** The plate is flexible, both the normal traction and displacement are not known.

i) **Bimaterial interface.** Two porous media are in contact with each other. The stress, displacement, pressure, and flux must be continuous across the interface, so there are eight conditions for a three-dimensional problem.

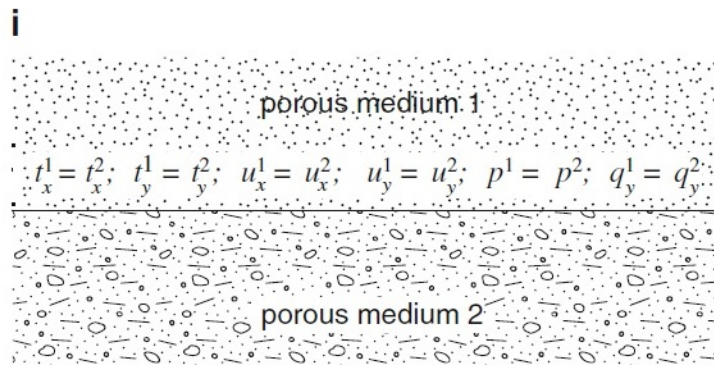
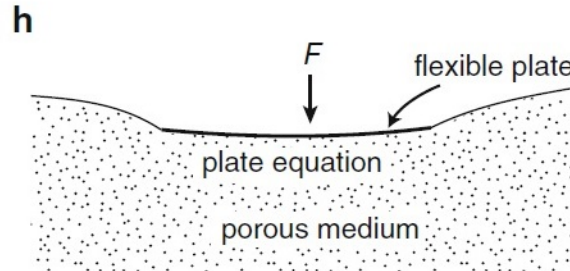
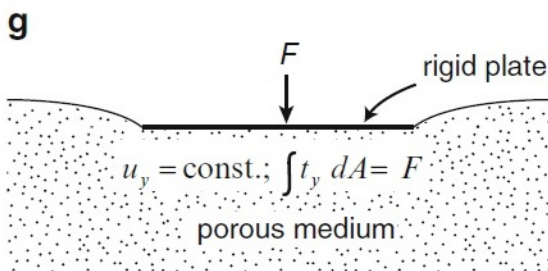
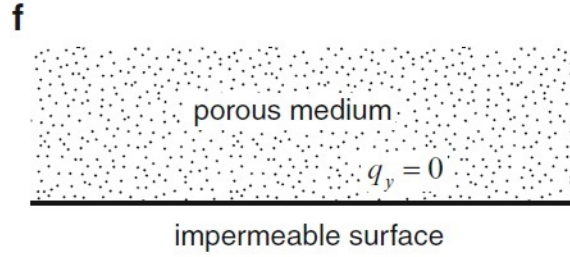
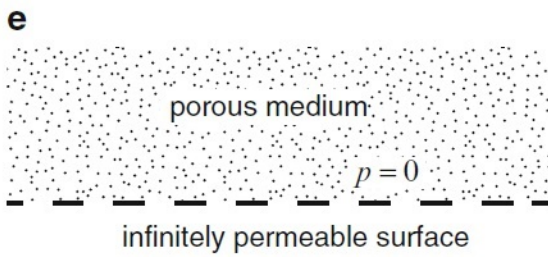
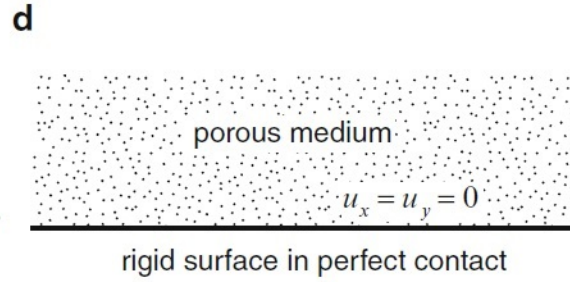
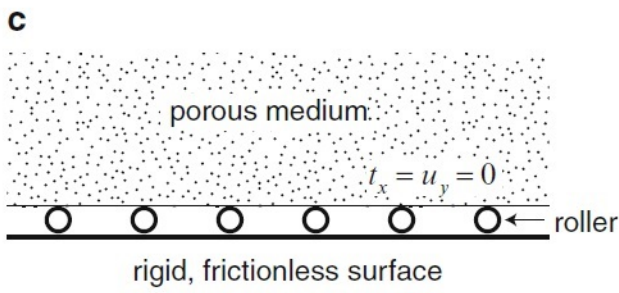
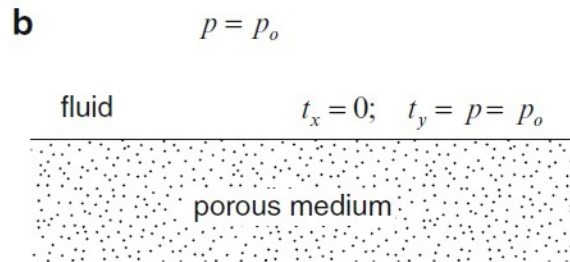
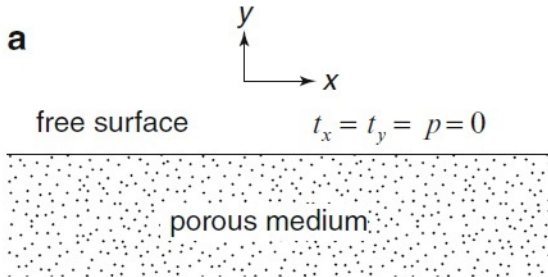


Figure 1.1: Types of physical boundary conditions (illustrated in two dimensions): (a) free surface, (b) fluid contact, (c) rigid, frictionless surface, (d) rigid surface in perfect contact (no slippage), (e) infinitely permeable surface, (f) impermeable surface, (g) rigid plate, (h) flexible plate, and (i) bimaterial interface

1.4.3. Diffusion in Poroelastic Media

A detailed mathematical analysis of poroelasticity is given by Showalter in [39]. Showalter developed the existence, uniqueness, and regularity theory for a general initial-boundary-value problem of poroelasticity. To that end, Showalter introduced the operator \mathcal{B} , $\mathcal{B}p = \nabla \cdot \mathbf{u}$, which allows him to write the equations as an implicit parabolic p.d.e. The operator \mathcal{B} is shown to be linear, continuous, monotone, and self-adjoint, and satisfy some properties on its range and kernel. Using this operator, the poroelasticity equations can be written as an implicit evolution equation. The main conclusions are based on results for Cauchy problems for implicit evolution equations of the type $\dot{\mathcal{B}}(\mathbf{u}) + \mathcal{A}(\mathbf{u}) = \mathbf{f}$, $t \in [0, T]$. Showalter showed that the poroelasticity equations have a unique strong solution and a weak solution, and that under additional mild assumptions, the weak solution is unique.

Governing equations

The poroelasticity system takes the form

$$-(\lambda + \mu)\nabla(\nabla \cdot \mathbf{u}) - \mu\Delta\mathbf{u} + \alpha\nabla p = \mathbf{f}, \quad (1.15)$$

and

$$\frac{\partial}{\partial t}(c_0 p + \alpha\nabla \cdot \mathbf{u}) - \nabla \cdot k\nabla p = h, \quad (1.16)$$

consisting of the equilibrium equation for conservation of momentum and the diffusion equation for the Darcy flow.

One characteristic of Showalter's paper is his treatment of boundary conditions. He considered two kinds of boundary conditions for both of the unknowns \mathbf{u} and p . For \mathbf{u} , the boundary is divided into a clamped portion Γ_c and a constraint on the complement Γ_t which involves the surface density of forces or traction $\sigma_{ij}n_j$,

$$\Gamma_c \cup \Gamma_t = \Gamma, \quad \Gamma_c \cap \Gamma_t = \{0\}, \quad (1.17)$$

and

$$u_i = 0 \text{ on } \Gamma_c, \quad \sigma_{ij}n_j = g_i \text{ on } \Gamma_t, \quad 1 \leq i \leq 3. \quad (1.18)$$

Similarly, The boundary conditions for p comprise of a homogeneous Dirichlet portion, also known as the drained portion of the boundary, and a portion Γ_f where the normal component of the flux is prescribed,

$$\Gamma_d \cup \Gamma_f = \Gamma, \quad \Gamma_d \cap \Gamma_f = \{0\}, \quad (1.19)$$

$$p = 0 \text{ on } \Gamma_d, \quad k \frac{\partial p}{\partial n_j} = h_1 \text{ on } \Gamma_f. \quad (1.20)$$

Showalter introduced the following operators in order to write the equations of poroelasticity more compactly. First, let $V = \{\mathbf{v} \in \mathbf{H}^1(\Omega) : \mathbf{v} = 0 \text{ on } \Gamma_c\}$, define the restriction to $C_0^\infty(\Omega)$ of $\mathcal{E}(\mathbf{u}) \in V'$ by $\mathcal{E}_0(\mathbf{u})$. Then

$$\mathcal{E}_0(\mathbf{u})_i = \frac{\partial a_{ijkl} \epsilon_{kl} \mathbf{u}}{\partial x_j}, \quad (1.21)$$

$$\mathcal{E}(\mathbf{u})(\mathbf{v}) = (\mathcal{E}_0(\mathbf{u}), \mathbf{v})_{L^2(\Omega)} + (a_{ijkl} \epsilon_{kl} \mathbf{u}, v_i)_{L^2(\Gamma_t)}, \quad \mathbf{v} \in V. \quad (1.22)$$

It can be seen that \mathcal{E} has been decoupled into the sum of its formal part \mathcal{E}_0 on Ω and its boundary part $\sigma_{ij} n_j$ on Γ_t . In this way the equations can be written concisely. Let Γ_s be the portion of the boundary on which neither pressure nor displacement are specified, $\Gamma_s = \Gamma_t \cap \Gamma_f$, then operators $\mathcal{A}, \vec{\nabla}, \vec{\nabla} \cdot$ can be defined

$$\mathcal{A}(p) = \left[A_0(p), k \frac{\partial p}{\partial n} \right] \in L^2(\Omega) \oplus L^2(\Gamma_f). \quad (1.23)$$

$$\vec{\nabla} p = [\nabla p, -\beta p \mathbf{n}] \in L^2(\Omega) \oplus L^2(\Gamma_s). \quad (1.24)$$

and

$$\vec{\nabla} \cdot \mathbf{v} = [\nabla \cdot \mathbf{v}, -(1 - \beta p) \mathbf{v} \cdot \mathbf{n}] \in L^2(\Omega) \oplus L^2(\Gamma_s). \quad (1.25)$$

With these operators, the quasi-static Cauchy problem can be written in the form

$$\begin{aligned} \mathcal{E}(\mathbf{u}(t)) + \alpha \vec{\nabla} p(t) &= \mathbf{f}(t), \\ \frac{d}{dt} \left(c_0 \mathcal{P}p(t) + \alpha \vec{\nabla} \cdot \mathbf{u}(t) \right) + \mathcal{A}p(t) &= h(t), \end{aligned} \quad (1.26)$$

and

$$c_0 \mathcal{P}p(0) + \alpha \vec{\nabla} \cdot \mathbf{u}(0) = [v_0, -v_1],$$

where $\mathcal{P} : L^2(\Omega) \oplus L^2(\Gamma_d) \rightarrow L^2(\Omega) \oplus \{0\}$ is the projection operator.

Strong solution

It is shown that this is a parabolic system which has a strong solution under minimal smoothness requirements on the initial data and source term. Showalter introduced an operator \mathcal{B} on $L^2(\Omega) \oplus L^2(\Gamma_s)$

$$\mathcal{B}p = \vec{\nabla} \cdot \mathbf{u}, \text{ where } \mathcal{E}(\mathbf{u}) = \vec{\nabla} p, \quad p = [f, g] \in L^2(\Omega) \oplus L^2(\Gamma_s). \quad (1.27)$$

The operator \mathcal{B} has the following properties

Lemma 1.1 *The operator $\mathcal{B} = -\vec{\nabla} \cdot \mathcal{E}^{-1} \vec{\nabla} : L^2(\Omega) \oplus L^2(\Gamma_s) \rightarrow L^2(\Omega) \oplus L^2(\Gamma_s)$ is continuous and self-adjoint with $\ker(\mathcal{B}) = \ker \vec{\nabla}$ and $\text{Im}(\mathcal{B}) = \ker \vec{\nabla}^\perp$, and each of the Sobolev spaces $(H^m(\Omega) \cap V) \oplus H^{m-1/2}(\Gamma_s)$ is invariant under \mathcal{B} .*

Written in terms of the operator \mathcal{B} , (1.26) has the form of an implicit evolution equation,

$$\frac{d}{dt} \left(c_0 \mathcal{P} + \mathcal{B} \right) p(t) + \mathcal{A}(p(t)) = h(t). \quad (1.28)$$

Using semi-group theory [10], [40], it is shown that this equation has a solution

Theorem 1.2 *Let $T > 0, v_0 \in L^2(\Omega), v_1 \in L^2(\Gamma_s)$, and the pair of Hölder continuous functions $h_0(\cdot) \in C^\alpha([0, T], L^2(\Omega))$, $h_1(\cdot) \in C^\alpha([0, T], L^2(\Gamma_s))$ be given with*

$$\int_{\Omega} v_0(x) dx - \int_{\Gamma_s} v_1(s) ds = 0, \quad (1.29)$$

and

$$\int_{\Omega} h_0(x, t) dx - \int_{\Gamma_s} h_1(s, t) ds = 0. \quad (1.30)$$

Then there exists a pair of functions $p(\cdot) : (0, T] \rightarrow V$ and $\mathbf{u}(\cdot) : (0, T] \rightarrow \mathbf{V}$ for which $c_0 p(\cdot) + \nabla \cdot \mathbf{u}(\cdot) \in C^0([0, T], L^2(\Omega)) \cap C^1((0, T], L^2(\Omega))$ and $(1 - \beta) \mathbf{u}(\cdot) \cdot \mathbf{n} \in C^0([0, T], L^2(\Gamma_s)) \cap C^1((0, T], L^2(\Gamma_s))$, and these satisfy the initial-boundary-value problem (1.26) with

$$t \rightarrow t \mathcal{A}(p(t)) = t \left[A_0(p(t)), k \frac{\partial p(t)}{\partial n} \right] \in L^\infty([0, T], L^2(\Omega) \oplus L^2(\Gamma_s)) \cap C^0((0, T], L^2(\Omega) \oplus L^2(\Gamma_s))$$

and

$$\int_{\Omega} (c_0 p(t) + \nabla \cdot \mathbf{u}(t)) dx - \int_{\Gamma_s} (1 - \beta) \mathbf{u}(t) \cdot \mathbf{n} ds = 0, \quad t \in (0, T]. \quad (1.31)$$

The function $\mathbf{u}(\cdot)$ is unique. When $\ker(c_0 \mathcal{P} + \mathcal{B} + \mathcal{A}) = \{0\}$, $p(\cdot)$ is unique, and if $\ker(c_0 \mathcal{P} + \mathcal{B}) \cap V = \{0\}$, the integral constraints (1.29), (1.30) and (1.31) are not necessary.

Weak solutions

Showalter also proved the existence and uniqueness of weak solutions.

Theorem 1.3 *Let $T > 0$, $v_0 \in V'_a$, and $h(\cdot) \in C^\alpha([0, T], V'_a)$ be given. Then there exists a unique pair of functions $p(\cdot) : (0, T] \rightarrow V$ and $\mathbf{u}(\cdot) : (0, T] \rightarrow \mathbf{V}$ for which $c_0 P p(\cdot) + \vec{\nabla} \cdot \mathbf{u}(\cdot) \in C^0([0, T], V'_a) \cap C^1([0, T], V'_a)$, and these satisfy the initial-value problem*

$$\begin{aligned} \mathcal{E}(\mathbf{u}(t)) + \alpha \vec{\nabla} p(t) &= 0, \\ \frac{d}{dt} \left(c_0 P p(t) + \alpha \vec{\nabla} \cdot \mathbf{u}(t) \right) + A p(t) &= h(t), \end{aligned} \quad (1.32)$$

and

$$\lim_{t \rightarrow 0^+} \left(c_0 P p(t) + \alpha \vec{\nabla} \cdot \mathbf{u}(t) \right) = v_0, \quad \text{in } V'_a.$$

1.4.4. Analysis of nonlinear poroelasticity

In [8], Cao, Chen, and Meir proved the existence and uniqueness of a solution and study the numerical approximation of solutions of nonlinear poroelasticity equations,

$$-(\lambda + \mu)\nabla(\nabla \cdot \mathbf{u}) - \mu\Delta\mathbf{u} + \alpha\nabla p = \mathbf{f}, \quad (1.33)$$

and

$$\frac{\partial}{\partial t}(c_0 p + \alpha\nabla \cdot \mathbf{u}) - \nabla \cdot (\kappa(\nabla \cdot \mathbf{u})\nabla p) = g, \quad (1.34)$$

subject to homogeneous boundary conditions. To that end, they applied a technique called the modified Rothe's method [47], which amounts to constructing a convergent sequence of approximate solutions using the backward Euler approximation of the time derivative. They also showed the convergence of a numerical method, using rigorous functional analysis arguments.

The main results of that work are the following theorems. They can be summarized as: the problem (1.33) – (1.34) has at least one solution, and under mild assumptions, the solution is unique. The error between the exact and numerical solutions can be bounded by the initial data and spatial discretization parameter h to the second order and time step size k to the first order.

Theorem 1.4 *Given $g \in L^2(I; L^2(\Omega))$, the problem (1.33)–(1.34) has at least one weak solution $(\mathbf{u}, p) \in L^2(I; H_0^1(\Omega)) \times L^2(I; H_0^1(\Omega))$.*

Theorem 1.5 *Assume that $\nabla p \in L^\infty(\Omega)$ and that there exists a constant C such that $\|\nabla p\|_{L^\infty(\Omega)} \leq C$, then the solution is unique.*

Theorem 1.6 *Assume that $p \in C^2(I; H^2(\Omega) \cap H_0^1(\Omega))$ and $\mathbf{u} \in C^1(I, W^{2,\infty}(\Omega))$, then for small enough time step k , there exist constants C_1 and C_2 which do not depend on k or discretization parameter h , such that*

$$\|\mathbf{u}^n - \mathbf{U}^n\| + \|p^n - P^n\| \leq C_1 \|l^0 - l\| + C_2(h^2 + k), \quad (1.35)$$

where \mathbf{U}^n and P^n are numerical approximations of solutions.

1.4.5. Seismic Phenomena in a Moist Soil

In this paper [12], Frenkel introduced the theory of wave propagation in saturated porous media. He first predicted and named a compressional wave, also known as the slow wave. Ivanov in 1939 [16] discovered that the propagation of elastic waves in the surface layers of the soil can cause the electrical response of the latter. This is because different positions from the source of the waves in th soil have different potentials. Ivanov called this the “seismoelectric effect of the second kind”. Frenkel explained this phenomenon as the result of second-type wave propagation. He started from the theory of Helmholtz and Smoluchovski that the differences of hydrostatic pressure Δp between two points of the soil must be connected with a difference of the electrical potential ²

$$\Delta V = \frac{\epsilon \zeta}{4\pi \mu \sigma} \Delta p$$

where ζ is the potential difference in the surface double layer, μ the viscosity of water and σ its electrical conductivity.

The author then discussed the elastic force acting on an unit volume of the soil, Φ , in different cases. For dry soil,

$$\Phi = (\lambda + \mu) \nabla(\nabla \cdot \mathbf{u}) + \mu \nabla^2 \mathbf{u}.$$

In the case of moist soil, the liquid phase is subjected to hydrostatic pressure p at all pores and p has the expression of

$$\frac{\Delta V}{V_1} = \frac{\Delta V_2}{V_2} = -\frac{1}{K_0} p,$$

where V_1 is the change of the volume of unit mass of the solid phase V_2 is the change of the volume of the pores, K_0 is the true compressibility modulus of the solid phase. After a series

²This assumption is actually incorrect, as pointed out by Pride in 1994 [34]. Since the Helmholtz-Smoluchowski equation assumes that the total electric current and an electrically driven conduction current in the porous media is everywhere zero. In fact, the total current should be present in the Ampère’s law.

of derivation, Φ now has the form of

$$\Phi = (\lambda + \mu)\nabla(\nabla \cdot \mathbf{u}) + \mu\nabla^2\mathbf{u} + K_2 \left(1 - \phi - \frac{K}{K_0}\right) \nabla p,$$

where K_2 is the compressibility modulus of the liquid. We can see that this expression is exactly the first equation of poroelasticity. When friction is taken into account, Darcy's equation will be used

$$\mathbf{v} = \frac{k}{\nu}(-\nabla p + \mathbf{F})$$

where \mathbf{F} denotes the external force acting on the liquid contained in a unit volume of the soil, ν the viscosity and k the filtration coefficient of the soil. Now terms of $\frac{\partial \mathbf{u}}{\partial t}$ serve as the elastic force Φ , the equation becomes

$$\rho_1 = (\lambda + \mu)\nabla(\nabla \cdot \mathbf{u}) + \mu\nabla^2\mathbf{u} + K_2 \left(1 - \phi - \frac{K}{K_0}\right) \nabla p + \frac{\nu}{\kappa} \left(\mathbf{v} - \frac{\partial \mathbf{u}}{\partial t}\right).$$

The author has also used methods in perturbation theory to analyze the propagation of longitudinal vibrations in the soil, a special case of longitudinal plane sine waves, and the propagation of traversal waves in a moist soil. Finally, he investigated the seismoelectric effect, with the help from the formula

$$\mathbf{E} = -\frac{\epsilon\zeta}{4\pi\mu\sigma} \frac{\partial p}{\partial x}.$$

He obtained

$$\mathbf{E} = C\mathbf{u},$$

where $C = \frac{2\epsilon\zeta\kappa\omega^2\phi\rho_2}{\pi\sigma r^2\mu} \left(\frac{K_2}{\rho_2} \frac{\beta}{\beta'w_0^2} - 1\right)$ can be regarded as a coefficient. Thus, though improperly given, the coupling effect of the electric field and the solid displacement has been described.

1.4.6. Governing equations for the electromagnetics and acoustics

We describe the model derived by Pride in [34]. Consider macroscopic dynamics of two-phase porous media possessing continuously distributed phases, Pride was the first to construct a model that correctly describes the interaction between mechanical waves and electric fields. He revised previous work of Frenkel [12] and Neev and Yeatts [27], and pointed out that they did not apply the full set of Maxwell’s equations which led to an erroneous conclusion. In practice, the fact that a macroscopic mechanical disturbance and an electromagnetic disturbance can excite each other constitutes the main finding of Pride’s paper, and it is one that Frenkel and Neev and Yeatts failed to realize.

A macroscopic mechanical disturbance can produce macroscopic electromagnetic disturbance, and vice versa.

When a macroscopic mechanical disturbance propagates through fluid saturated porous media, a packing of grains saturated by electrolytes for instance, a small amount of relative motion is induced between the fluid and solid phases. This relative motion will carry along the excess ions in the electric double layers near the grain surfaces. In this way, the effect of a mechanical wave resembles that caused by a current source for a macroscopic electromagnetic disturbance. Conversely, an electromagnetic disturbance can serve a similar function as a macroscopic mechanical disturbance. That is because when a macroscopic electromagnetic disturbance propagates, the charge excess of the double layers will be influenced by an electric field hence a pressure gradient in the fluid is generated and, in principle, a macroscopic mechanical disturbance.

Boundary conditions

The boundary conditions for Pride’s model are prescribed on the boundaries called “shear plane”. We first introduce the adsorbed layer and “diffuse layer”, and the shear plane which separates one from another. The adsorbed layer is a layer of electrolyte ions and structured water molecules that are chemically and physically adsorbed by the surface of the solid grains. This layer also includes the ionized surface sites present on the grain surfaces. The molecules and ions in this layer are assumed to be immobile. The diffuse layer is the region

of fluid adjacent to the adsorbed layer. If there is a net excess of charge in the adsorbed layer, it is balanced by an opposite amount of excess mobile ions distributed in the diffuse layer. The complex structure of the shear plane, therefore, makes the boundary conditions defined on it impossible to use for calculations.

Next we will introduce the model derived by Pride.

Pore and grain-scale governing equations

A. Electromagnetic equations

The electromagnetic equations that will be used to derive the final coupled equations are

$$\nabla \cdot \mathbf{B}_s = 0, \quad (1.36)$$

$$\nabla \cdot \mathbf{D}_s = 0, \quad (1.37)$$

$$\nabla \times \mathbf{E}_s = -\dot{\mathbf{B}}_s, \quad (1.38)$$

$$\nabla \times \mathbf{H}_s = \dot{\mathbf{D}}_s, \quad (1.39)$$

$$\nabla \cdot \mathbf{B}_f = 0, \quad (1.40)$$

$$\nabla \cdot \mathbf{D}_f = \sum_{l=1}^L ez_l N_l, \quad (1.41)$$

$$\nabla \times \mathbf{E}_f = -\dot{\mathbf{B}}_f, \quad (1.42)$$

$$\nabla \times \mathbf{H}_f = \dot{\mathbf{D}}_f + \mathbf{J}_f, \quad (1.43)$$

$$\mathbf{J}_f = \sum_{l=1}^L ez_l [-kTb_l \nabla N_l + ez_l b_l N_l \mathbf{E}_f + N_l \dot{\mathbf{u}}_f], \quad (1.44)$$

$$\mathbf{B}_\xi = \mu_0 \mathbf{H}_\xi, \quad (1.45)$$

and

$$\mathbf{D}_\xi = \epsilon_0 \kappa_\xi \mathbf{E}_\xi. \quad (1.46)$$

Equations (1.36) – (1.39) and (1.40) – (1.43) are Maxwell’s equations for the solid and fluid phases, respectively. The ionic-current density \mathbf{J}_f has contributions from the diffusion, electromigration, and convection of ions. $\dot{\mathbf{u}}_f$ is the instantaneous fluid velocity. The ionic properties are the valences z_l (ez_l represents the net charge and sign on each species- l ion), the number densities N_l , and the mobilities b_l .

The boundary conditions are (on the shear plane)

$$\mathbf{n} \cdot (\mathbf{B}_s - \mathbf{B}_f) = \mathbf{0}, \quad (1.47)$$

$$\mathbf{n} \cdot (\mathbf{D}_s - \mathbf{D}_f) = Q, \quad (1.48)$$

$$\mathbf{n} \times (\mathbf{E}_s - \mathbf{E}_f) = Q\dot{\mathbf{u}}_s, \quad (1.49)$$

$$\mathbf{n} \times (\mathbf{H}_s - \mathbf{H}_f) = \mathbf{0}, \quad (1.50)$$

and

$$\mathbf{n} \cdot \mathbf{J}_f = \dot{Q}. \quad (1.51)$$

The boundary conditions (1.47) and (1.48) are the same as the boundary conditions of Maxwell's equations. There is a jump, “ Q ”, for the electrical displacement \mathbf{D} across the boundary but the magnetic field \mathbf{B} will be continuous. The boundary condition (1.49) has a nonzero right hand side induced by movement of the solid, and the boundary condition (1.50) is homogeneous, because of the absence of steady currents. Equation (1.51) is obtained by taking the divergence of Ampère's law and the time derivative of Coulomb's law.

Pride assumes that the disturbances are time-harmonic, and that all field variables can be written in the form of

$$Q(t) = Q^0 + \text{Re}\{q(\omega)e^{-i\omega t}\}, \quad (1.52)$$

$$N_l(t) = N_l^0 + \text{Re}\{n_l(\omega)e^{-i\omega t}\}, \quad (1.53)$$

and

$$\mathbf{E}_f(t) = \mathbf{E}_f^0 + \text{Re}\{\mathbf{e}_f(\omega)e^{-i\omega t}\}. \quad (1.54)$$

B. Mechanical equations

The mechanical equations for the displacements \mathbf{u}_s and \mathbf{u}_f are

$$-i\omega\rho_f\dot{\mathbf{u}}_f = \nabla \cdot \tau_f + \sum_{l=1}^L ez_l(N_l^0\mathbf{e}_f + n_l\mathbf{E}_f^0), \quad (1.55)$$

$$-i\omega\rho_s\dot{\mathbf{u}}_s = \nabla \cdot \tau_s, \quad (1.56)$$

$$\mathbf{u}_f = K_f\nabla \cdot \mathbf{u}_f\mathbf{I} - i\omega\eta(\nabla\mathbf{u}_f + \nabla\mathbf{u}_f^T - \frac{2}{3}\nabla \cdot \mathbf{u}_f\mathbf{I}), \quad (1.57)$$

and

$$\mathbf{u}_s = K_s\nabla \cdot \mathbf{u}_s\mathbf{I} + G(\nabla\mathbf{u}_s + \nabla\mathbf{u}_s^T - \frac{2}{3}\nabla \cdot \mathbf{u}_s\mathbf{I}), \quad (1.58)$$

Equations (1.55) and (1.56) describe that the dynamics of both the fluid and solid phases are governed by the conservation of linear momentum. The nonlinear convective term $\dot{\mathbf{u}} \cdot \nabla \mathbf{u}$ has been ignored in (1.57) and (1.58), as justified in [35]. The boundary conditions are

$$\mathbf{n} \cdot (\tau_s - \tau_f) = -Q^0\mathbf{e}_s, \quad (1.59)$$

and

$$\mathbf{u}_s - \mathbf{u}_f = 0. \quad (1.60)$$

On the normal direction of the boundary, a difference between the fluid and solid stress tensors has been induced by the electric field, the right-hand side of (1.59) represents the electrical body force acting on the excess charge of the adsorbed layer. The right-hand side of (1.60) is obviously zero, if we recall the \mathbf{u}_s and \mathbf{u}_f are the solid and fluid displacements, respectively.

C. Transport coefficients

Pride carefully determines the expressions for the coefficients $\sigma(\omega)$, the electrical conductivity, $L(\omega)$, the coupling coefficient and $k(\omega)$, the permeability. [They are calculated], not measured. In summary,

$$\sigma(\omega) = \frac{\phi\sigma_f}{\alpha_\infty} \left[1 + \frac{2[C_{em} + C_{os}(\omega)]}{\sigma_f\Lambda} \right], \quad (1.61)$$

$$L(\omega) = L_0 \left[1 - i \frac{\omega}{\omega_t} \frac{m}{4} \left(1 - 2 \frac{\tilde{d}}{\Lambda} \right)^2 \left(1 - i^{3/2} \tilde{d} \sqrt{\frac{\omega\rho_f}{\eta}} \right)^2 \right]^{-\frac{1}{2}} \quad (1.62)$$

and

$$k(\omega) = \left[\left(1 - i \frac{\omega}{\omega_t} \frac{4}{m} \right)^{\frac{1}{2}} - i \frac{\omega}{\omega_t} \right]^{-1}, \quad (1.63)$$

where the forms of the tortuosity α_∞ , the porosity ϕ , the excess conductance associated with the electromigration of double layer ions C_{em} , the conductance due to electrically induced streaming of the ions C_{os} , the fluid density ρ_f , the conductivity σ_f , the transition frequency ω_t , the dimensionless number m , the low-frequency coupling coefficient L_0 and the dc permeability k_0 can be found in [34]. In [38], there is a table that shows the values of these coefficients in three different materials.

D. The final form of the macroscopic governing equations

In summary, Pride's equations can be written as

$$\nabla \times \mathbf{E} = i\omega\mathbf{B}, \quad (1.64)$$

$$\nabla \times \mathbf{H} = -i\omega\mathbf{D} + \mathbf{J}, \quad (1.65)$$

$$\nabla \cdot \tau_B = -\omega^2(\rho_B\mathbf{u}_s + \rho_f\mathbf{w}), \quad (1.66)$$

$$\mathbf{J} = \sigma(\omega)\mathbf{E} + L(\omega)(-\nabla p + \omega^2\rho_f\mathbf{u}_s), \quad (1.67)$$

$$-i\omega\mathbf{w} = L(\omega)\mathbf{E} + \frac{k(\omega)}{\eta}(-\nabla p + \omega^2\rho_f\mathbf{u}_s), \quad (1.68)$$

$$\mathbf{D} = \epsilon_0 \left[\frac{\phi}{\alpha_\infty}(\kappa_f - \kappa_s) + \kappa_s \right] \mathbf{E}, \quad (1.69)$$

$$\mathbf{B} = \mu_0\mathbf{H}, \quad (1.70)$$

$$\tau_B = (K_G\nabla \cdot \mathbf{u}_s + C\nabla \cdot \mathbf{w})\mathbf{I} + G_{fr} \left(\nabla\mathbf{u}_s + \nabla\mathbf{u}_s^T - \frac{2}{3}\nabla \cdot \mathbf{u}_s\mathbf{I} \right), \quad (1.71)$$

and

$$-p = C\nabla \cdot \mathbf{u}_s + M\nabla \cdot \mathbf{w}. \quad (1.72)$$

We will derive a quasi-static model based on these equations, and impose boundary conditions on the boundary of the domain.

1.4.7. Numerical electroseismic modeling: A finite element approach

The equations of porous media under the influence of electromagnetic waves were derived by Pride in [34] where the author also determined the expression of the various coefficients. Santos et al. [38] study these equations and derive a method for approximating the solutions. They proved the uniqueness of the solution, discretized the equations in both space and time and discussed element selections. We will describe some of their work, and at the same time, provide some comments.

The differential model

Santos et al. follow [34] and [15] and write the equations as follows. Consider a 3D rectangular domain $\Omega = \Omega_a \cup \Omega_p$ where Ω_a and Ω_p are associated with the air and subsurface poroelastic (disjoint) parts of Ω , respectively. The equations are

$$\epsilon \frac{\partial \mathbf{E}}{\partial t} + \sigma \mathbf{E} - \nabla \times \mathbf{H} = \mathbf{J}_e^s, \quad \text{in } \Omega, \quad (1.73)$$

$$\nabla \times \mathbf{E} + \mu \frac{\partial \mathbf{H}}{\partial t} = \mathbf{0}, \quad \text{in } \Omega, \quad (1.74)$$

$$\rho_b \frac{\partial^2 \mathbf{u}^s}{\partial t^2} + \rho_f \frac{\partial^2 \mathbf{u}^f}{\partial t^2} - \nabla \cdot \boldsymbol{\tau} = \mathbf{F}^{(s)}, \quad \text{in } \Omega_p, \quad (1.75)$$

$$\rho_f \frac{\partial^2 \mathbf{u}^s}{\partial t^2} + m \frac{\partial^2 \mathbf{u}^f}{\partial t^2} + \frac{\eta}{\kappa_0} \frac{\partial \mathbf{u}^f}{\partial t} - L_0 \frac{\eta}{\kappa_0} \mathbf{E} + \nabla p = \mathbf{F}^{(f)}, \quad \text{in } \Omega_p, \quad (1.76)$$

$$2G\epsilon_{lm}(\mathbf{u}^s) + \delta_{lm}(\lambda_c \nabla \cdot \mathbf{u}^s + \alpha K_{av} \nabla \cdot \mathbf{u}^f) = \tau_{lm}(\mathbf{u}), \quad \text{in } \Omega_p, \quad (1.77)$$

and

$$-\alpha K_{av} \nabla \cdot \mathbf{u}^s - K_{av} \nabla \cdot \mathbf{u}^f = p, \quad \text{in } \Omega_p. \quad (1.78)$$

Comparing these equations and those of Pride there is a term missing in equation (1.73), that is, the term $-L_0 \nabla p$ should also be on the left side. Recall the main conclusion of Pride's

paper, “When a macroscopic mechanical disturbance propagates through a porous material, a small amount of relative motion is induced between the fluid and solid phases. This relative flow will carry along the excess ions in the electric double layers near the grain surfaces. Thus, a mechanical wave can act as a current source for macroscopic-electromagnetic disturbances. Similarly, when an electromagnetic disturbance propagates, the electric field will act on the charge excesses of the double layers producing pressure gradients in the fluid and, in principle, macroscopic-mechanical disturbances”. Simply ignoring the coupling term $-L_0\nabla p$ in Maxwell’s equations violates the spirit of Pride’s paper. However, mathematically, the discussion in [38] is still of interest and relevant to our work.

In [46], the author has given an explanation of dropping the coupling term $-L_0\nabla p$. He first described the fact that the electrokinetic mobility L provides coupling between the EM system and mechanical system (Biot’s equations). The author uses perturbation methods to study the full system. He assumes weak coupling so that to leading order, i.e. the zeroth order in L , the EM system field satisfies the conventional Maxwell’s equations ($L = 0$). Then the Maxwell’s equations can be solved independently, and, the coupling term only presents as a source in the mechanical equations.

Here we keep the coupling term $-L_0\nabla p$ for several reasons. First, we are studying the well-posedness of the full system, and provide a theoretical background for using finite element methods, we don’t need to sacrifice accuracy for simplicity. Second, the author in [46] does not suggest any mathematical, physical, or experimental arguments to support this idea of dropping the coupling term. Third, dropping the coupling term is not consistent with Pride’s statements. Finally, in [46] the author refers to some experiments ([30], [44]) which, do not include a justification for dropping the coupling term in the EM system, but not in the mechanical system. Therefore, we keep this coupling term.

Santos et al. proposed boundary conditions on the boundary of the domain Ω . These conditions can be used in mathematical computation. The authors introduced the quantities

$$\mathcal{G}_{\Gamma_s}(\mathbf{u}) = \begin{pmatrix} \tau(\mathbf{u})\mathbf{n} \cdot \mathbf{n} \\ \tau(\mathbf{u})\mathbf{n} \cdot \chi^1 \\ \tau(\mathbf{u})\mathbf{n} \cdot \chi^2 \\ p \end{pmatrix}, \quad \mathcal{S}_{\Gamma_s}(\mathbf{u}) = \begin{pmatrix} \mathbf{u}^s \cdot \mathbf{n} \\ \mathbf{u}^s \cdot \chi^1 \\ \mathbf{u}^s \cdot \chi^2 \\ \mathbf{u}^f \cdot \mathbf{n}, \end{pmatrix} \quad (1.79)$$

where χ^1 and χ^2 are two unit tangent vectors on the boundary such that $\{\mathbf{n}, \chi^1, \chi^2\}$ is an orthonormal set. Define

$$P_\chi \mathbf{E} = \mathbf{E} - \mathbf{n}(\mathbf{n} \cdot \mathbf{E}) = -\mathbf{n} \times \mathbf{n} \times \mathbf{E} \quad (1.80)$$

which is the 3-D orthogonal projection of the trace of E onto the tangent plane perpendicular to the normal vector \mathbf{n} . Then the boundary conditions are

$$\sqrt{\epsilon} P_\chi \mathbf{E} + \sqrt{\mu} \mathbf{n} \times \mathbf{H} = 0, \quad \text{on } \Gamma, \quad (1.81)$$

$$-\mathcal{G}_{\Gamma_p}(\mathbf{u}) = \mathcal{D} \mathcal{S}_{\Gamma_p} \left(\frac{\partial \mathbf{u}}{\partial t} \right), \quad \text{on } \Gamma_p, \quad (1.82)$$

and

$$-\mathcal{G}_{\Gamma_p}(\mathbf{u}) = 0, \quad \text{on } \Gamma_{a,p}. \quad (1.83)$$

Here, the matrix \mathcal{D} is introduced so that the boundary conditions can be written compactly.

Its definition is $\mathcal{D} = \mathcal{R}^{\frac{1}{2}} \mathcal{S}^{\frac{1}{2}} \mathcal{R}^{\frac{1}{2}}$, where $\mathcal{S} = \mathcal{R}^{-\frac{1}{2}} \mathcal{M} \mathcal{R}^{-\frac{1}{2}}$ and $b = \rho_b - \frac{(\rho_f)^2}{m}$,

$$\mathcal{R} = \begin{pmatrix} \rho_b & 0 & 0 & \rho_f \\ 0 & b & 0 & 0 \\ 0 & 0 & b & 0 \\ \rho_f & 0 & 0 & m \end{pmatrix}, \quad \mathcal{M} = \begin{pmatrix} \lambda_c + 2G & 0 & 0 & \alpha K_{av} \\ 0 & G & 0 & 0 \\ 0 & 0 & G & 0 \\ \alpha K_{av} & 0 & 0 & K_{av} \end{pmatrix}. \quad (1.84)$$

Here \mathcal{D} is a coefficient matrix, so are the matrices \mathcal{S} , \mathcal{R} , \mathcal{M} .

Weak formulation, existence and uniqueness of solutions.

The weak formulation is: for $t \in [0, T]$, find $(\mathbf{E}, \mathbf{H}, \mathbf{u}^s, \mathbf{u}^f)(t) \in H(\text{curl}, \Omega) \times [L^2(\Omega)]^3 \times [H^1(\Omega)]^3 \times H(\text{div}, \Omega)$ such that:

$$\left(\epsilon \frac{\partial \mathbf{E}}{\partial t}, \psi \right) + (\sigma \mathbf{E}, \psi) - (\mathbf{H}, \nabla \times \psi) + \left\langle \sqrt{\frac{\epsilon}{\mu}} P_\chi \mathbf{E}, P_\chi \psi \right\rangle = (\mathbf{J}_e^s, \psi),$$

$$\psi \in H(\text{curl}, \Omega), \quad (1.85)$$

$$(\nabla \times \mathbf{E}, \varphi) + \left(\mu \frac{\partial \mathbf{H}}{\partial t}, \varphi \right) = \mathbf{0}, \quad \varphi \in [L^2(\Omega)]^3, \quad (1.86)$$

and

$$\begin{aligned} & \left(\mathcal{P} \frac{\partial^2 \mathbf{u}}{\partial t^2}, \mathbf{v} \right) + \left(\frac{\eta}{\kappa_0} \frac{\partial \mathbf{u}^f}{\partial t}, \mathbf{v}^f \right) + \mathcal{A}(u, v) \\ & - \left(L_0 \frac{\eta}{\kappa_0} \mathbf{E}, \mathbf{v}^f \right) + \left\langle \mathcal{D} \mathcal{S}_{\Gamma_p} \left(\frac{\partial \mathbf{u}^f}{\partial t} \right), \mathcal{S}_{\Gamma_p}(\mathbf{v}) \right\rangle = 0, \\ & \mathbf{v} = (\mathbf{v}^s, \mathbf{v}^f) \in [H^1(\Omega_p)]^3 \times H(\text{div}, \Omega_p). \end{aligned} \quad (1.87)$$

where $\langle \cdot, \cdot \rangle$ represents the boundary integral. In (1.87)

$$\mathcal{P} = \begin{pmatrix} \rho_b I_d & \rho_f I_d \\ \rho_f I_d & m I_d \end{pmatrix}, \quad (1.88)$$

where I_d is the identity matrix in $\mathbb{R}^{d \times d}$ and $\mathcal{A}(u, v)$ is the bilinear form defined by:

$$\mathcal{A}(u, v) = \sum_{l,m} (\tau_{lm}(\mathbf{u}), \varepsilon_{lm}(\mathbf{v}^s))_{\Omega_p} - (p, \nabla \cdot \mathbf{v}^f)_{\Omega_p}. \quad (1.89)$$

Letting $\psi = \mathbf{E}$, $\varphi = \mathbf{H}$, $\mathbf{v}^s = \frac{\partial \mathbf{u}^s}{\partial t}$, $\mathbf{v}^f = \frac{\partial \mathbf{u}^f}{\partial t}$, adding the resulting equations together, Santos et al get that the norms of the unknowns are bounded by initial data, where the uniqueness of solution is implied.

It is claimed that the uniqueness can be obtained using the compactness argument of Lions [19] with an argument similar to that given in [37], so a detailed proof is omitted. It

seems that the existence issue is much more complicated than uniqueness. A rigorous proof is needed.

A continuous-time finite element method. Parallelepiped elements. A priori error estimates.

After choosing parallelepiped elements, Santos et al. showed that the solution is unique, and derive the following error estimate:

$$\begin{aligned}
& \|\mathbf{E} - \mathbf{E}^h\|_\infty + \|\mathbf{H} - \mathbf{H}^h\|_\infty + \|\mathbf{u}^s - \mathbf{u}^{s,h}\|_\infty + \|\mathbf{u}^f - \mathbf{u}^{f,h}\|_\infty \\
+ & \left\| \frac{\partial(\mathbf{u}^s - \mathbf{u}^{s,h})}{\partial t} \right\|_\infty + \left\| \frac{\partial(\mathbf{f}^s - \mathbf{u}^{f,h})}{\partial t} \right\|_\infty + \|\mathbf{u}^s - \mathbf{u}^{s,h}\|_2 + \|(\mathbf{u}^s - \mathbf{u}^{s,h}) \cdot \mathbf{v}\|_\infty \\
\leq & Ch^{1/2}[N_0 + N_1 + M_0 + M_1], \tag{1.90}
\end{aligned}$$

where C is some constant independent of h , N_0 , N_1 , M_0 and M_1 [are sum of some of] $\|\mathbf{E}\|^2$, $\|\mathbf{H}\|^2$, $\|\mathbf{u}^s\|^2$, $\|\mathbf{u}^f\|^2$.

A discrete-time finite element method. Tetrahedral elements.

For a discrete-time finite element method and the case of tetrahedral elements, the uniqueness and existence of solutions and a priori estimates are also obtained.

They also provide a chart of physical parameters,

	Homogeneous region	Layer 1: brine saturated	Layer 2: 75% gas – 25% brine saturation
$\sigma^c(S/m)$	0.01	0.1	0.001
$\phi(-)$	0.2	0.25	0.2
$K_s(Pa)$	3.7×10^{10}	2.5×10^{10}	3.7×10^{10}
$v_s(m/s)$	1400	1450	1800
$\rho_s(kg/m^3)$	2650	2650	2650
$k_0(m^2)$	10^{-13}	10^{-16}	10^{-13}
$L_0(A/(Pa \cdot m))$	3.2×10^{-15}	1.5×10^{-9}	3.3×10^{-9}
$\rho_f(kg/m^3)$	1000	1000	0.88
$\eta(kg/(m \cdot s))$	0.001	0.001	1×10^{-5}
$K_f(Pa)$	2.25×10^9	2.25×10^9	0.1×10^9
$S_f(-)$	1	1	0.75

Chapter 2

Model

2.1. Governing Equation

We use the full-time version of Pride's equations. There are three sources of force that drive the charges to produce the current \mathbf{J} : the electromagnetic field, pressure gradient, and elastic waves. The coupling term included in the equation that governs the solid-fluid relative speed - the speed is also determined by the electric field, in addition to pressure and solid displacement as we see from poroelasticity equations. The coupling effect is linear, so the linearity of the whole system of equations is preserved. The equations are

$$\epsilon \frac{\partial \mathbf{E}}{\partial t} - \nabla \times \mathbf{H} = -\mathbf{J}, \quad (2.1)$$

$$\mu \frac{\partial \mathbf{H}}{\partial t} + \nabla \times \mathbf{E} = 0, \quad (2.2)$$

$$\nabla \cdot \tau_B = \frac{\partial^2}{\partial t^2} (\rho_B \mathbf{u}_s + \rho_f \mathbf{w}), \quad (2.3)$$

$$\mathbf{J} = \sigma \mathbf{E} + L \left(-\nabla p - \rho_f \frac{\partial^2 \mathbf{u}_s}{\partial t^2} \right), \quad (2.4)$$

$$\frac{\partial \mathbf{w}}{\partial t} = L \mathbf{E} + \frac{k}{\eta} \left(-\nabla p - \rho_f \frac{\partial^2 \mathbf{u}_s}{\partial t^2} \right), \quad (2.5)$$

$$\tau_B = (K_G \nabla \cdot \mathbf{u}_s + C \nabla \cdot \mathbf{w}) \mathbf{I} + G_{fr} (\nabla \mathbf{u}_s + \nabla \mathbf{u}_s^T - \frac{2}{3} \nabla \cdot \mathbf{u}_s \mathbf{I}), \quad (2.6)$$

and

$$-p = C \nabla \cdot \mathbf{u}_s + M \nabla \cdot \mathbf{w}. \quad (2.7)$$

Here \mathbf{E} is the electric field, \mathbf{H} is the magnetic field, τ_B is the bulk stress tensor, \mathbf{J} is the current density, \mathbf{u}_s is the displacement of the solid matrix, $\mathbf{w} = \phi(\mathbf{u}_f - \mathbf{u}_s)$ is the relative fluid-solid displacement, \mathbf{u}_f is the displacement of the fluid, and p is the pressure in the

fluid. These are the unknowns. In addition, the physical parameters which appear above are ϵ the electric permittivity and μ the magnetic permeability of the material, ϕ the porosity, ρ_s the solid density, ρ_f the fluid density, and $\rho_B = \phi\rho_f + (1 - \phi)\rho_s$ the bulk density, k the permeability, η the fluid's shear viscosity, σ the electrical conductivity, L a frequency dependent coupling coefficient, C the bulk-electrolyte molarity, and G_{fr} the shear moduli of the framework (matrix). Finally $K_G = \frac{K_{fr} + \phi K_f + (1 + \phi)K_s\Delta}{1 + \Delta}$ and $M = \frac{1}{\phi} \frac{K_f}{1 + \Delta}$, where K_{fr} is the bulk moduli of the solid frame when the fluid is a gas or is absent, K_f and K_s are the bulk moduli of the fluid and solid, respectively, and $\Delta = \frac{K_f}{\phi K_s} [(1 - \phi)K_s - K_{fr}]$. Also above, \mathbf{I} is the identity tensor.

The equations are posed on a spatial domain Ω . Here Ω is an open, bounded, simply connected, subset of \mathbb{R}^3 with a Lipschitz continuous boundary $\partial\Omega$.

We simplify the system and convert it to quasi-static equations. Eliminating \mathbf{J} we have

$$\epsilon \frac{\partial \mathbf{E}}{\partial t} + \sigma \mathbf{E} - \nabla \times \mathbf{H} - L(\nabla p + \rho_f \frac{\partial^2 \mathbf{u}_s}{\partial t^2}) = 0, \quad (2.8)$$

$$\mu \frac{\partial \mathbf{H}}{\partial t} + \nabla \times \mathbf{E} = 0, \quad (2.9)$$

$$\frac{\partial^2}{\partial t^2} (\rho_B \mathbf{u}_s + \rho_f \mathbf{w}) - \nabla \cdot \boldsymbol{\tau}_B = 0, \quad (2.10)$$

$$\frac{\partial \mathbf{w}}{\partial t} - L \mathbf{E} + \frac{k}{\eta} (\nabla p - \rho_f \frac{\partial^2 \mathbf{u}_s}{\partial t^2}) = 0, \quad (2.11)$$

$$(K_G \nabla \cdot \mathbf{u}_s + C \nabla \cdot \mathbf{w}) \mathbf{I} + G_{fr} (\nabla \mathbf{u}_s + \nabla \mathbf{u}_s^T - \frac{2}{3} \nabla \cdot \mathbf{u}_s \mathbf{I}) = \boldsymbol{\tau}_B, \quad (2.12)$$

and

$$C \nabla \cdot \mathbf{u}_s + M \nabla \cdot \mathbf{w} = -p. \quad (2.13)$$

Substituting (2.12) into (2.10) yields

$$\epsilon \frac{\partial \mathbf{E}}{\partial t} + \sigma \mathbf{E} - \nabla \times \mathbf{H} - L(\nabla p - \rho_f \frac{\partial^2 \mathbf{u}_s}{\partial t^2}) = 0, \quad (2.14)$$

$$\mu \frac{\partial \mathbf{H}}{\partial t} + \nabla \times \mathbf{E} = 0, \quad (2.15)$$

$$\frac{\partial^2}{\partial t^2} (\rho_B \mathbf{u}_s + \rho_f \mathbf{w}) - [G \nabla \cdot \nabla \mathbf{u}_s + (K_G + \frac{1}{3}G) \nabla (\nabla \cdot \mathbf{u}_s) + C \nabla (\nabla \cdot \mathbf{w})] = 0, \quad (2.16)$$

$$\frac{\partial \mathbf{w}}{\partial t} - L \mathbf{E} + \frac{k}{\eta} (\nabla p - \rho_f \frac{\partial^2 \mathbf{u}_s}{\partial t^2}) = 0, \quad (2.17)$$

and

$$p + C \nabla \cdot \mathbf{u}_s + M \nabla \cdot \mathbf{w} = 0. \quad (2.18)$$

Ignoring the second order time derivatives we get

$$\epsilon \frac{\partial \mathbf{E}}{\partial t} + \sigma \mathbf{E} - \nabla \times \mathbf{H} - L \nabla p = 0,$$

$$\mu \frac{\partial \mathbf{H}}{\partial t} + \nabla \times \mathbf{E} = 0,$$

$$-[G \nabla \cdot \nabla \mathbf{u}_s + (K_G + \frac{1}{3}G) \nabla (\nabla \cdot \mathbf{u}_s) + C \nabla (\nabla \cdot \mathbf{w})] = 0,$$

$$\frac{\partial \mathbf{w}}{\partial t} - L \mathbf{E} + \frac{k}{\eta} \nabla p = 0,$$

and

$$p + C \nabla \cdot \mathbf{u}_s + M \nabla \cdot \mathbf{w} = 0.$$

Finally, eliminating \mathbf{w} and letting $\mathbf{u}_s = \mathbf{u}$, $K_G + \frac{1}{3}G - \frac{C^2}{M} = \lambda_c$, $\frac{C}{M} = \alpha$, $\frac{1}{M} = c_0$ and $\frac{k}{\eta} = \kappa$, the equations can be written as

$$\epsilon \frac{\partial \mathbf{E}}{\partial t} + \sigma \mathbf{E} - \nabla \times \mathbf{H} - L \nabla p = 0, \quad (2.19)$$

$$\mu \frac{\partial \mathbf{H}}{\partial t} + \nabla \times \mathbf{E} = 0, \quad (2.20)$$

$$-\lambda_c \nabla (\nabla \cdot \mathbf{u}) - G \nabla \cdot \nabla \mathbf{u} + \alpha \nabla p = 0, \quad (2.21)$$

and

$$\frac{\partial}{\partial t} (c_0 p + \alpha \nabla \cdot \mathbf{u}) + L \nabla \cdot \mathbf{E} - \kappa \Delta p = 0. \quad (2.22)$$

2.2. Initial and Boundary Conditions

We supplement the system of equations with initial conditions: at $t = 0$,

$$\mathbf{E}(\mathbf{x}, 0) = \mathbf{E}_0(\mathbf{x}), \quad \mathbf{H}(\mathbf{x}, 0) = \mathbf{H}_0(\mathbf{x}), \quad \text{and} \quad (c_0 p + \alpha \nabla \cdot \mathbf{u})(\mathbf{x}, 0) = l(\mathbf{x}), \quad \text{in } \Omega. \quad (2.23)$$

For simplicity we assume a perfect conducting boundary which yields the a boundary condition for the electric field

$$\mathbf{E} \times \mathbf{n} = \mathbf{0}, \quad \text{on } \partial\Omega \times (0, T],$$

(where as usual \mathbf{n} denotes the unit, outward pointing, normal vector to Ω) and homogeneous Dirichlet boundary condition for the displacement and pressure, namely,

$$\mathbf{u} = \mathbf{0} \quad \text{and} \quad p = 0, \quad \text{on } \partial\Omega \times (0, T].$$

Remark Nonhomogeneous boundary conditions, as well as other types boundary conditions can also be considered. The analysis for nonhomogeneous Dirichlet boundary conditions can be performed using the the proposed methodology (while the analysis for other types of boundary conditions will be considered elsewhere).

2.3. Weak Form of the Governing Equations

Using L^2 -based Sobolev spaces (spaces that are now considered standard, see [23] and references cited therein for definitions, inner products and norms on these spaces, and for notation used), we introduce the weak formulation for the system under consideration (2.20)–(2.22).

Recall the integration by parts formulas

$$(\nabla \times \mathbf{U}, \mathbf{V}) - (\mathbf{U}, \nabla \times \mathbf{V}) = \langle \mathbf{U} \times \mathbf{n}, \mathbf{V} \rangle, \quad \mathbf{U}, \mathbf{V} \in H(\text{curl}, \Omega),$$

and

$$(\nabla \cdot \mathbf{U}, V) + (\mathbf{U}, \nabla V) = \langle \mathbf{U} \cdot \mathbf{n}, V \rangle, \quad \mathbf{U} \in H(\text{div}, \Omega), V \in H^1(\Omega).$$

Let $I = (0, T]$, $\mathbb{D} = L^2(I; H_0(\text{curl}, \Omega)) \cap H^1(I; L^2(\Omega))$, $\mathbb{B} = L^2(I; L^2(\Omega)) \cap H^1(I; L^2(\Omega))$, $\mathbb{V} = L^2(I; H_0^1(\Omega)) \cap H^1(I; L^2(\Omega))$, $\mathbb{Q} = L^2(I; H_0^1(\Omega)) \cap H^1(I; H^{-1}(\Omega))$. The weak formulation of the problem is: find $(\mathbf{E}, \mathbf{H}, \mathbf{u}, p) \in \mathbb{D} \times \mathbb{B} \times \mathbb{V} \times \mathbb{Q}$ that satisfies (2.23) such that for a.e. $t \in (0, T]$:

$$\left(\epsilon \frac{\partial \mathbf{E}}{\partial t}, \mathbf{D} \right) + (\sigma \mathbf{E}, \mathbf{D}) - (\mathbf{H}, \nabla \times \mathbf{D}) - (L \nabla p, \mathbf{D}) = 0, \quad \forall \mathbf{D} \in \mathbb{D}, \quad (2.24)$$

$$\left(\mu \frac{\partial \mathbf{H}}{\partial t}, \mathbf{B} \right) + (\nabla \times \mathbf{E}, \mathbf{B}) = 0, \quad \forall \mathbf{B} \in \mathbb{B}, \quad (2.25)$$

$$(\lambda_c \nabla \cdot \mathbf{u}, \nabla \cdot \mathbf{v}) + (G \nabla \mathbf{u}, \nabla \mathbf{v}) + (\alpha \nabla p, \mathbf{v}) = 0, \quad \forall \mathbf{v} \in \mathbb{V}, \quad (2.26)$$

and

$$\left(c_0 \frac{\partial p}{\partial t}, q \right) + \left(\alpha \frac{\partial (\nabla \cdot \mathbf{u})}{\partial t}, q \right) - (L \mathbf{E}, \nabla q) + (\kappa \nabla p, \nabla q) = 0, \quad \forall q \in \mathbb{Q}. \quad (2.27)$$

We recall that (\cdot, \cdot) denotes the L^2 inner product (in space) and $\|\cdot\|$ denotes the corresponding L^2 norm (other norms are denoted with respective subscripts), additionally we use the same notation for spaces, inner products, and norms of scalar and vector valued functions, the meaning being obvious from the context.

2.4. A Priori Estimates

Letting $\mathbf{B} = \mathbf{H}$ in (2.25), we get

$$\left(\mu \frac{\partial \mathbf{H}}{\partial t}, \mathbf{H} \right) + (\nabla \times \mathbf{E}, \mathbf{H}) = 0. \quad (2.28)$$

Also, let $\mathbf{D} = \mathbf{E}$ in (2.24) and use (2.28) to obtain

$$\left(\epsilon \frac{\partial \mathbf{E}}{\partial t}, \mathbf{E} \right) + (\sigma \mathbf{E}, \mathbf{E}) + \left(\mu \frac{\partial \mathbf{H}}{\partial t}, \mathbf{H} \right) - (L \nabla p, \mathbf{E}) = 0. \quad (2.29)$$

Next, choose $\mathbf{v} = \frac{\partial \mathbf{u}}{\partial t}$ in (2.26), $q = p$ in (2.27)

$$\left(\alpha p, \frac{\partial \nabla \cdot \mathbf{u}}{\partial t} \right) = \left(\lambda_c \nabla \cdot \mathbf{u}, \frac{\partial \nabla \cdot \mathbf{u}}{\partial t} \right) + \left(G \nabla \mathbf{u}, \frac{\partial \nabla \mathbf{u}}{\partial t} \right), \quad (2.30)$$

and add the resulting equation to (2.29) to get

$$\begin{aligned} \frac{1}{2} \frac{d}{dt} \left[(\epsilon \mathbf{E}, \mathbf{E}) + (\mu \mathbf{H}, \mathbf{H}) + (c_0 p, p) \right] + (\sigma \mathbf{E}, \mathbf{E}) + \left(\alpha \frac{\partial \nabla \cdot \mathbf{u}}{\partial t}, p \right) \\ - 2(L \nabla p, E) + (\kappa \nabla p, \nabla p) = 0. \end{aligned} \quad (2.31)$$

substituting (2.30) into (2.31) yields

$$\begin{aligned} \frac{1}{2} \frac{d}{dt} \left[(\epsilon \mathbf{E}, \mathbf{E}) + (\mu \mathbf{H}, \mathbf{H}) + (\lambda_c \nabla \cdot \mathbf{u}, \nabla \cdot \mathbf{u}) + (G \nabla \mathbf{u}, \nabla \mathbf{u}) + (c_0 p, p) \right] \\ - 2(L \nabla p, E) + (\sigma \mathbf{E}, \mathbf{E}) + (\kappa \nabla p, \nabla p) = 0. \end{aligned} \quad (2.32)$$

Integrating in time,

$$\begin{aligned} \frac{1}{2} \left[(\epsilon \mathbf{E}, \mathbf{E}) + (\mu \mathbf{H}, \mathbf{H}) + (\lambda_c \nabla \cdot \mathbf{u}, \nabla \cdot \mathbf{u}) + (G \nabla \mathbf{u}, \nabla \mathbf{u}) + (c_0 p, p) \right] \\ + \int_0^T (\sigma \mathbf{E}, \mathbf{E}) dt - \int_0^T 2(L \nabla p, E) dt + \int_0^T (\kappa \nabla p, \nabla p) dt \\ = \frac{1}{2} \left[(\epsilon \mathbf{E}_0, \mathbf{E}_0) + (\mu \mathbf{H}_0, \mathbf{H}_0) + (\lambda_c \nabla \cdot \mathbf{u}_0, \nabla \cdot \mathbf{u}_0) \right. \\ \left. + (G \nabla \mathbf{u}_0, \nabla \mathbf{u}_0) + (c_0 p_0, p_0) \right]. \end{aligned} \quad (2.33)$$

Or equivalently,

$$\begin{aligned} \frac{1}{2} \left[\epsilon \|\mathbf{E}\|^2 + \mu \|\mathbf{H}\|^2 + \lambda_c \|\nabla \cdot \mathbf{u}\|^2 + G \|\nabla \mathbf{u}\|^2 + c_0 \|p\|^2 \right] \\ \leq \frac{1}{2} \left[\epsilon \|\mathbf{E}_0\|^2 + \mu \|\mathbf{H}_0\|^2 + \lambda_c \|(\nabla \cdot \mathbf{u})_0\|^2 + G \|(\nabla \mathbf{u})_0\|^2 + c_0 \|p_0\|^2 \right] \end{aligned}$$

Since ϵ and μ are electromagnetic constants, they are bounded below and above by some positive constants,

$$0 < \epsilon_* \leq \epsilon \leq \epsilon^* < \infty, \quad 0 < \mu_* \leq \mu \leq \mu^* < \infty. \quad (2.34)$$

and the fact that L is minuscule ($3.2 \times 10^{-15} \sim 1.5 \times 10^{-9} A/(Pa \cdot m)$) compared to σ ($0.1 \sim 0.001 S/m$) and κ ($10^{-10} \sim 10^{-8} m^3 \cdot s/kg$), the sum of the integrals $\int_0^T (\sigma \mathbf{E}, \mathbf{E}) dt - \int_0^T 2(L \nabla p, E) dt + \int_0^T (\kappa \nabla p, \nabla p) dt$ is always positive.

Applying Gronwall's lemma [36], notifying that all terms on the left-hand side of (2.34) are nonnegative and bounded by initial data, we conclude our problem has at most one solution, given the condition

$$L^2 < \sigma \kappa, \quad (2.35)$$

where this is satisfied by real world materials.

2.5. The Operator \mathcal{B}

We express \mathbf{u} also in terms of p so we can study an equation that has three variables explicitly.

Define a bilinear form

$$a(\mathbf{u}, \mathbf{v}) := (\lambda_c + G)(\nabla \cdot \mathbf{u}, \nabla \cdot \mathbf{v}) + \mu(\nabla \mathbf{u}, \nabla \mathbf{v}), \quad \text{for all } \mathbf{u}, \mathbf{v} \in H_0^1(\Omega). \quad (2.36)$$

It is easy to verify that the bilinear form $a(\cdot, \cdot)$ is continuous and coercive on $H_0^1(\Omega) \times H_0^1(\Omega)$. Define the associated operator $\mathcal{B} : L^2(\Omega) \rightarrow L^2(\Omega)$ such that for $q \in L^2(\Omega)$, $\mathcal{B}q := \nabla \cdot \mathbf{u}$ where \mathbf{u} satisfies

$$a(\mathbf{u}, \mathbf{v}) = (\nabla q, \mathbf{v}), \quad \text{for all } \mathbf{v} \in \mathbf{H}_0^1(\Omega),$$

and

$$\mathbf{u} = 0, \quad \text{on } \partial\Omega.$$

The proofs of the properties of the operator \mathcal{B} can be found in [39]. The operator \mathcal{B} defined above is linear, continuous, monotone, and self-adjoint, with $\ker(\mathcal{B}) = \ker(\nabla)$ and $\text{range}(\mathcal{B}) = \ker(\nabla)^\perp$. Moreover, $\ker(\mathcal{B}) = \ker(\nabla) = \{0\}$ because of the homogeneous boundary condition. Hence B is a continuous bijection from $L^2(\Omega)$ into itself. According to the bounded inverse theorem, \mathcal{B} and also $c_0 + \mathcal{B}$ have bounded inverses.

Chapter 3

Numerical approximation

We now consider numerical approximation of the solutions of the initial value problem (2.24) – (2.27).

We start by constructing appropriate finite element spaces. Let T_h be a family of quasi-uniform triangulations (into triangles or tetrahedra), see [42], of the polygonal, or polyhedral, domain Ω satisfying $\max_{\tau \in T_h} \text{diam}(\tau) \leq h$ (where τ is a geometrical element, and h is the mesh parameter). Let $\{P_j\}_{j=1}^{N_h}$ be the set of all the interior nodes of the triangulation (where N_h is the number of interior nodes). Following [23], let \mathbb{P}_r denote the standard space of polynomials of total degree less than or equal to r , and let $\tilde{\mathbb{P}}_r$ denote the space of homogeneous polynomials of order r . Let $\mathbb{S}_r = \{\mathbf{p} \in (\tilde{\mathbb{P}}_r)^3 : \mathbf{p}(\mathbf{x}) \cdot \mathbf{x} = 0, \mathbf{x} \in \mathbb{R}^3\}$, then define $\mathbb{R}_r = (\mathbb{P}_{r-1})^3 \oplus \mathbb{S}_r$. Let $\mathbb{H}_h = \{\mathbf{B} \in L^2(\Omega) : \mathbf{B}|_\tau \in (\mathbb{P}_{r-1})^3, \forall \tau \in T_h\}$, and $\mathbb{E}_h = \{\mathbf{D} \in H(\text{curl}, \Omega) : \mathbf{D}|_\tau \in \mathbb{R}_r, \forall \tau \in T_h\}$. In other words, the space \mathbb{E}_h is the space of Nédélec edge elements whose standard notation is $N1_r^e$. Let \mathbb{Q}_h be the space consisting of continuous functions on Ω which are polynomials of order r on each triangle, or tetrahedron, and vanish on $\partial\Omega$ that is $\mathbb{Q}_h = \{p \in C(\Omega) : p|_\tau \in \mathbb{P}_r, \forall \tau \in T_h\}$ i.e., for $r = 1$ or 2 , this is the usual space of linear or quadratic Lagrange elements that vanish on the boundary). Denote by Φ_j the piecewise polynomial of order r which is 1 at P_j and vanishes at all the other nodes. It is easy to see that $\{\Phi_j\}_{j=1}^{N_h}$ forms a basis of \mathbb{Q}_h . Let $\mathbb{V}_h = (\mathbb{Q}_h)^3$, then $\{(\Phi_j, 0, 0), (0, \Phi_j, 0), (0, 0, \Phi_j)\}_{j=1}^{N_h}$ forms a basis of $(\mathbb{Q}_h)^3$.

Denote the time step size by k , that is, $k = T/N$ for some positive integer N , and $t_n = nk$ for $n = 0, 1, \dots, N$. Define $\Delta^- P^n = P^n - P^{n-1}$ for $n = 1, 2, \dots, N$. The fully discrete approximation is: find $\mathbf{e}^n \in \mathbb{E}_h$, $\mathbf{h}^n \in \mathbb{H}_h$, $\mathbf{U}^n \in \mathbb{V}_h$ and $P^n \in \mathbb{Q}_h$ for $n = 1, 2, \dots, N$, such that

$$k^{-1}\Delta^-(\epsilon\mathbf{e}^n, \mathbf{d}) + (\sigma\mathbf{e}^n, \mathbf{d}) - (\mathbf{h}^n, \nabla \times \mathbf{d}) - (L\nabla P^n, \mathbf{d}) = 0, \quad \forall \mathbf{d} \in \mathbb{E}_h, \quad (3.1)$$

$$k^{-1}\Delta^-(\mu\mathbf{h}^n, \mathbf{b}) + (\nabla \times \mathbf{e}^n, \mathbf{b}) = 0, \quad \forall \mathbf{b} \in \mathbb{H}_h, \quad (3.2)$$

$$a(\mathbf{U}^n, \mathbf{V}) + (\nabla P^n, \mathbf{V}) = 0, \quad \forall \mathbf{V} \in \mathbb{V}_h, \quad (3.3)$$

$$k^{-1}\Delta^-(c_0P^n, Q) + k^{-1}\Delta^-(\nabla \cdot \mathbf{U}^n, Q) - (L\mathbf{e}^n, \nabla Q) + (\kappa\nabla P^n, \nabla Q) = 0, \quad \forall Q \in \mathbb{Q}_h, \quad (3.4)$$

Here we set $c_0P^0 + \nabla \cdot \mathbf{U}^0 = l_0$, where l_0 is an approximation to l in \mathbb{Q}_h .

Remark The existence of a weak solution of (3.1)–(3.4) can be shown by using an argument similar to the one which was used for the continuous problem.

We now consider error estimates for the approximate solution given by (3.1)–(3.4). That is, we provide an estimates for the difference between the solution of (3.1)–(3.4) (approximate solution) and that of (2.24)–(2.27) (exact solution). We use Ritz-Galerkin like projections of the solution of (2.24)–(2.27). Given $p \in H_0^1(\Omega)$, define the projection \mathcal{R}_hp of p onto \mathbb{Q}_h as follows

$$(\kappa\nabla(p - \mathcal{R}_hp), \nabla q) = 0, \quad \forall q \in \mathbb{Q}_h. \quad (3.5)$$

We need the following results to estimate the error of \mathbf{E} and \mathbf{H} . For any $\tau \in T_h$ and $\mathbf{E} \in W^{1,m}(\Omega)$, $m > 2$, we can define the interpolation operator $\mathcal{I}_h\mathbf{E} \in \mathbb{E}_h$ such that $\mathcal{I}_h\mathbf{E}|_\tau \in \mathbb{E}_h$ has the same moments as \mathbf{E} on τ , the definition of moments we use is the same as in [17]. The error estimate for interpolation can be found in [26].

Lemma 3.1 *Let $1 \leq m \leq r$, if $\mathbf{E} \in H^{m+1}(\Omega)$, then there exists a constant C such that*

$$\|\mathbf{E} - \mathcal{I}_h\mathbf{E}\| + \|\nabla \times (\mathbf{E} - \mathcal{I}_h\mathbf{E})\| \leq Ch^m\|\mathbf{E}\|_{m+1}.$$

The error estimate for projection can be found in [25].

Lemma 3.2 *Define the projection $\mathcal{P}_H : L^2(\Omega) \rightarrow \mathbb{H}_h$ as in [25]:*

$$(\mathbf{H} - \mathcal{P}_H \mathbf{H}, \mathbf{B}) = 0, \quad \forall \mathbf{B} \in \mathbb{H}_h.$$

Then if $\mathbf{H} \in H^m(\Omega)$ for $0 \leq m \leq r$, there exists a constant C such that

$$\|\mathbf{H} - \mathcal{P}_H \mathbf{H}\| \leq Ch^m \|\mathbf{H}\|_m, \quad 0 \leq m \leq k.$$

The initial conditions used in the approximation are the interpolant and projection of the exact initial conditions respectively,

$$\mathbf{E}^n(0) = \mathcal{I}_h \mathbf{E}_0, \quad \mathbf{H}^n(0) = \mathcal{P}_H \mathbf{H}_0. \quad (3.6)$$

Also needed are some estimates on the time derivative. Writing $\mathbf{U}^i = \mathbf{U}(t_i)$, and letting \mathbb{X} be $H^1(\text{curl}, \Omega)$ or $H^\alpha(\Omega)$, $\alpha \geq 0$, then from [17]

Lemma 3.3 *We have that*

$$\left\| \frac{\partial \mathbf{U}^i}{\partial t} \right\|_{\mathbb{X}}^2 \leq \frac{1}{k} \int_{t^{i-1}}^{t^i} \|\mathbf{U}_t\|_{\mathbb{X}}^2 dt, \quad \forall \mathbf{U} \in H^1(I; \mathbb{X}).$$

Additionally from [18]

Lemma 3.4 *We have that*

$$\left\| \mathbf{U}^i - \frac{1}{k} \int_{I^i} \mathbf{U} dt \right\|_{\mathbb{X}}^2 \leq k \int_{I^i} \|\mathbf{U}_t\|_{\mathbb{X}}^2 dt, \quad \forall \mathbf{U} \in H^1(I; \mathbb{X}),$$

and

$$\left\| \mathbf{U}^{i-1} - \frac{1}{k} \int_{I^i} \mathbf{U} dt \right\|_{\mathbb{X}}^2 \leq k \int_{I^i} \|\mathbf{U}_t\|_{\mathbb{X}}^2 dt, \quad \forall \mathbf{U} \in H^1(I; \mathbb{X}).$$

We will also make use of the lemmas 3.5 – 3.8 which can be found in [42] and [33].

Lemma 3.5 *Let \mathcal{B} be a continuous linear operator on a Banach space X and let $f : [0, T] \rightarrow X$ be continuously differentiable with respect to t . Then $\mathcal{B} \frac{\partial f}{\partial t} = \frac{\partial}{\partial t} \mathcal{B} f$.*

Lemma 3.6 *Let \mathbb{Q}_h be given as above. Define the interpolation operator $\mathcal{I}_h : H^{r+1}(\Omega) \cap H_0^1(\Omega) \rightarrow \mathbb{Q}_h$. For any $q \in H^{r+1}(\Omega) \cap H_0^1(\Omega)$, and $1 \leq m \leq r+1$*

$$\|q - \mathcal{I}_h q\| + h \|\nabla(q - \mathcal{I}_h q)\| \leq Ch^m \|q\|_m.$$

To estimate the difference (error) between p^n and P^n , we define

$$\delta^n := p^n - \mathcal{R}_h p^n \quad \text{and} \quad \theta^n := \mathcal{R}_h p^n - P^n. \quad (3.7)$$

With these we can write the difference between p^n and P^n as

$$p^n - P^n = \delta^n + \theta^n. \quad (3.8)$$

Lemma 3.7 *Assume that $q \in H^{r+1}(\Omega) \cap H_0^1(\Omega)$. Then there exists a constant C such that*

$$\|q - \mathcal{R}_h q\| + h \|\nabla(q - \mathcal{R}_h q)\| \leq Ch^m \|q\|_m, \quad \text{for } 1 \leq m \leq r+1$$

Lemma 3.8 *Assume that $p \in C^1(I : H^{r+1}(\Omega) \cap H_0^1(\Omega))$. Then there exists a constant C such that*

$$\|\delta(t)\| + h \|\nabla \delta(t)\| \leq C(p) h^m, \quad \text{for } 1 \leq m \leq r+1, \quad t \in (0, T]$$

and

$$\|\delta_t(t)\| + h \|\nabla \delta_t(t)\| \leq C(p, p_t) h^m, \quad \text{for } 1 \leq m \leq r+1, \quad t \in (0, T].$$

We are now ready to derive the estimates for the solution of (3.1)–(3.4).

Theorem 3.9 *Assume that $\mathbf{E} \in H^{m+1}(\Omega)$, $p \in C^1(I; H^m(\Omega) \cap H_0^1(\Omega))$ and $\mathbf{u} \in C^1(I, H^m(\Omega))$, then there exists $k_0 > 0$ such that for $k \leq k_0$, there exist constants C_1 and C_2 which do not depend on h or k , such that*

$$\|\mathbf{E}^n - \mathbf{e}^n\| + \|\mathbf{H}^n - \mathbf{h}^n\| + \|\mathbf{u}^n - \mathbf{U}^n\| + \|p^n - P^n\| \leq C_1 \|l^0 - l\| + C_2(h^m + k), \quad (3.9)$$

Proof:

We start by expressing \mathbf{u} in terms of p using the operator \mathcal{B} , then equations (2.26) and (2.27) in weak formulation will have the form of

$$\left((c_0 + \mathcal{B}) \frac{\partial p}{\partial t}, q \right) - (L\mathbf{E}, \nabla q) + (\kappa \nabla p, \nabla q) = 0, \quad \forall q \in \mathbb{Q}, \quad (3.10)$$

and equations (3.3) and (3.4) are combined as

$$k^{-1} \Delta^-((c_0 + \mathcal{B})P^i, Q) - (L\mathbf{e}^i, \nabla Q) + (\kappa \nabla P^i, \nabla Q) = 0, \quad \forall Q \in \mathbb{Q}_h. \quad (3.11)$$

Multiplying the weak equations (2.24), (2.25), and (3.10) by $1/k$, integrating over I^i , $i = 1, 2, \dots, N$, and choosing $\mathbf{D} = \mathbf{d}$, $\mathbf{B} = \mathbf{b}$, and $q = Q$ yields

$$\begin{aligned} & \frac{\epsilon}{k} (\mathbf{E}^i - \mathbf{E}^{i-1}, \mathbf{d}) + \frac{\sigma}{k} \left(\int_{I^i} \mathbf{E}(\tau) d\tau, \mathbf{d} \right) \\ & - \frac{1}{k} \left(\int_{I^i} \mathbf{H}(\tau) d\tau, \nabla \times \mathbf{d} \right) - \frac{L}{k} \left(\int_{I^i} \nabla p(\tau) d\tau, \mathbf{d} \right) = 0, \quad \forall \mathbf{d} \in \mathbb{D}, \end{aligned} \quad (3.12)$$

$$\frac{\mu}{k} (\mathbf{H}^i - \mathbf{H}^{i-1}, \mathbf{b}) + \left(\nabla \times \frac{1}{k} \int_{I^i} \mathbf{E}(\tau) d\tau, \mathbf{b} \right) = 0, \quad \forall \mathbf{b} \in \mathbb{B}. \quad (3.13)$$

and

$$\frac{1}{k} \left((c_0 + \mathcal{B})(p^i - p^{i-1}), Q \right) - L \left(\int_{I^i} \mathbf{E}(\tau) d\tau, \nabla Q \right) + \kappa \left(\int_{I^i} \nabla p(\tau) d\tau, \nabla Q \right) = 0, \quad \forall Q \in \mathbb{Q}. \quad (3.14)$$

Subtracting (3.12) from (3.1), (3.13) from (3.2), and (3.14) from (3.11), we obtain the error equations

$$\begin{aligned} & \epsilon(k^{-1}\Delta^-(\mathbf{E}^i - \mathbf{e}^i), \mathbf{d}) + \sigma\left(\frac{1}{k}\int_{I^i}\mathbf{E}(\tau)d\tau - \mathbf{e}^i, \mathbf{d}\right) \\ & - \left(\frac{1}{k}\int_{I^i}\mathbf{H}(\tau)d\tau - \mathbf{h}^i, \nabla \times \mathbf{d}\right) - L\left(\frac{1}{k}\int_{I^i}\nabla p(\tau)d\tau - \nabla p^i, \mathbf{d}\right) = 0, \quad \mathbf{d} \in \mathbb{D}_h, \end{aligned} \quad (3.15)$$

$$\mu(k^{-1}\Delta^-(\mathbf{H}^i - \mathbf{h}^i), \mathbf{b}) + \left(\nabla \times \left(\frac{1}{k}\int_{I^i}\mathbf{E}(\tau)d\tau - \mathbf{e}^i\right), \mathbf{b}\right) = 0, \quad \mathbf{b} \in \mathbb{B}_h. \quad (3.16)$$

$$\begin{aligned} & \left(k^{-1}\Delta^-(c_0 + \mathcal{B})(p^i - P^i), Q\right) - L\left(\frac{1}{k}\int_{I^i}\mathbf{E}(\tau)d\tau - \mathbf{e}^i, \nabla Q\right) \\ & + \kappa\left(\frac{1}{k}\int_{I^i}\nabla p(\tau)d\tau - \nabla P^i, \nabla Q\right) = 0, \quad Q \in \mathbb{Q}_h. \end{aligned} \quad (3.17)$$

Choosing $\mathbf{d} = \mathcal{I}_h\mathbf{E}^i - \mathbf{e}^i$ in (3.15), $\mathbf{b} = \mathcal{P}_H\mathbf{H}^i - \mathbf{h}^i$ in (3.16), and $Q = \mathcal{R}_hp^i - P^i$ in (3.17) we can rewrite these as

$$\begin{aligned} & \epsilon(k^{-1}\Delta^-(\mathcal{I}_h\mathbf{E}^i - \mathbf{e}^i), \mathcal{I}_h\mathbf{E}^i - \mathbf{e}^i) - (\mathcal{P}_H\mathbf{H}^i - \mathbf{h}^i, \nabla \times (\mathcal{I}_h\mathbf{E}^i - \mathbf{e}^i)) \\ & = \epsilon(k^{-1}\Delta^-(\mathcal{I}_h\mathbf{E}^i - \mathbf{E}^i), \mathcal{I}_h\mathbf{E}^i - \mathbf{e}^i) - \sigma\left(\frac{1}{k}\int_{I^i}\mathbf{E}(\tau)d\tau - \mathcal{I}_h\mathbf{E}^i, \mathcal{I}_h\mathbf{E}^i - \mathbf{e}^i\right) \\ & - \sigma(\mathcal{I}_h\mathbf{E}^i - \mathbf{e}^i, \mathcal{I}_h\mathbf{E}^i - \mathbf{e}^i) - (\mathcal{P}_H\mathbf{H}^i - \mathbf{H}^i, \nabla \times (\mathcal{I}_h\mathbf{E}^i - \mathbf{e}^i)) \\ & - \left(\mathbf{H}^i - \frac{1}{k}\int_{I^i}\mathbf{H}(\tau)d\tau, \nabla \times (\mathcal{I}_h\mathbf{E}^i - \mathbf{e}^i)\right) + L\left(\frac{1}{k}\int_{I^i}\nabla p(\tau)d\tau - \nabla p^i, \mathcal{I}_h\mathbf{E}^i - \mathbf{e}^i\right), \end{aligned} \quad (3.18)$$

$$\begin{aligned} & \mu(k^{-1}\Delta^-(\mathcal{P}_H\mathbf{H}^i - \mathbf{h}^i), \mathcal{P}_H\mathbf{H}^i - \mathbf{h}^i) + (\nabla \times (\mathcal{I}_h\mathbf{E}^i - \mathbf{e}^i), \mathcal{P}_H\mathbf{H}^i - \mathbf{h}^i) \\ & = \mu(k^{-1}\Delta^-(\mathcal{P}_H\mathbf{H}^i - \mathbf{H}^i), \mathcal{P}_H\mathbf{H}^i - \mathbf{h}^i) + (\nabla \times (\mathcal{I}_h\mathbf{E}^i - \mathbf{E}^i), \mathcal{P}_H\mathbf{H}^i - \mathbf{h}^i) \\ & + \left(\nabla \times \left(\mathbf{E}^i - \frac{1}{k}\int_{I^i}\mathbf{E}(\tau)d\tau\right), \mathcal{P}_H\mathbf{H}^i - \mathbf{h}^i\right) \end{aligned} \quad (3.19)$$

$$\begin{aligned} & (k^{-1}\Delta^-(c_0 + \mathcal{B})(\mathcal{R}_hp^i - P^i), \mathcal{R}_hp^i - P^i) \\ & = (k^{-1}\Delta^-(c_0 + \mathcal{B})(\mathcal{R}_hp^i - p^i), \mathcal{R}_hp^i - P^i) + L\left(\frac{1}{k}\int_{I^i}\mathbf{E}(\tau)d\tau - \mathbf{e}^i, \nabla(\mathcal{R}_hp - P^i)\right) \\ & - \kappa\left(\frac{1}{k}\int_{I^i}\nabla p(\tau)d\tau - \nabla\mathcal{R}_hp^i, \nabla(\mathcal{R}_hp - P^i)\right) - \kappa\left(\nabla(\mathcal{R}_hp - P)^i, \nabla(\mathcal{R}_hp - P)^i\right). \end{aligned} \quad (3.20)$$

Now adding the three equations together, multiplying the resulting equation by k , and using the fact that

$$\frac{1}{2}(a^2 - b^2) \leq a(a - b), \quad \forall a, b \in \mathbb{R}, \quad (3.21)$$

we have

$$\begin{aligned}
& \epsilon(\Delta^-(\mathcal{I}_h \mathbf{E}^i - \mathbf{e}^i), \mathcal{I}_h \mathbf{E}^i - \mathbf{e}^i) + \mu(\Delta^-(\mathcal{P}_H \mathbf{H}^i - \mathbf{h}^i), \mathcal{P}_H \mathbf{H}^i - \mathbf{h}^i) \\
& + (\Delta^-(c_0 + \mathcal{B})(\mathcal{R}_h p^i - P^i), \mathcal{R}_h p^i - P^i) \\
\leq & \epsilon k(k^{-1} \Delta^-(\mathcal{I}_h \mathbf{E}^i - \mathbf{E}^i), \mathcal{I}_h \mathbf{E}^i - \mathbf{e}^i) - \sigma k \left(\frac{1}{k} \int_{I^i} \mathbf{E}(\tau) d\tau - \mathcal{I}_h \mathbf{E}^i, \mathcal{I}_h \mathbf{E}^i - \mathbf{e}^i \right) \\
& - \sigma k (\mathcal{I}_h \mathbf{E}^i - \mathbf{e}^i, \mathcal{I}_h \mathbf{E}^i - \mathbf{e}^i) - k (\mathcal{P}_H \mathbf{H}^i - \mathbf{H}^i, \nabla \times (\mathcal{I}_h \mathbf{E}^i - \mathbf{e}^i)) \\
& - k \left(\mathbf{H}^i - \frac{1}{k} \int_{I^i} \mathbf{H}(\tau) d\tau, \nabla \times (\mathcal{I}_h \mathbf{E}^i - \mathbf{e}^i) \right) + \mu k(k^{-1} \Delta^-(\mathcal{P}_H \mathbf{H}^i - \mathbf{H}^i), \mathcal{P}_H \mathbf{H}^i - \mathbf{h}^i) \\
& + k (\nabla \times (\mathcal{I}_h \mathbf{E}^i - \mathbf{E}^i), \mathcal{P}_H \mathbf{H}^i - \mathbf{h}^i) + k \left(\nabla \times \left(\mathbf{E}^i - \frac{1}{k} \int_{I^i} \mathbf{E}(\tau) d\tau \right), \mathcal{P}_H \mathbf{H}^i - \mathbf{h}^i \right) \\
& + k(k^{-1} \Delta^-(c_0 + \mathcal{B})(\mathcal{R}_h p^i - p^i), \mathcal{R}_h p^i - P^i) - \kappa k \left(\frac{1}{k} \int_{I^i} \nabla p(\tau) d\tau - \nabla \mathcal{R}_h p^i, \nabla(\mathcal{R}_h p - P)^i \right) \\
& - \kappa k (\nabla(\mathcal{R}_h p - P)^i, \nabla(\mathcal{R}_h p - P)^i) + Lk \left(\frac{1}{k} \int_{I^i} \nabla p(\tau) d\tau - \nabla p^i, \mathcal{I}_h \mathbf{E}^i - \mathbf{e}^i \right) \\
& + Lk \left(\frac{1}{k} \int_{I^i} \mathbf{E}(\tau) d\tau - \mathbf{e}^i, \nabla(\mathcal{R}_h p - P)^i \right) \quad (3.22)
\end{aligned}$$

We first give an estimate to the sum of the last two terms from inequality (3.22) using the condition (2.35), which is $\sigma\kappa - L^2 > 0$. This is performed by using Young's inequality

$$\begin{aligned}
& Lk \left(\frac{1}{k} \int_{I^i} \nabla p(\tau) d\tau - \nabla p^i, \mathcal{I}_h \mathbf{E}^i - \mathbf{e}^i \right) + Lk \left(\frac{1}{k} \int_{I^i} \mathbf{E}(\tau) d\tau - \mathbf{e}^i, \nabla(\mathcal{R}_h p - P)^i \right) \\
\leq & \frac{\kappa}{8} k \left\| \frac{1}{k} \int_{I^i} \nabla p(\tau) d\tau - \nabla p^i \right\|^2 + 2\sigma k \|\mathcal{I}_h \mathbf{E}^i - \mathbf{e}^i\|^2 \\
& + \frac{\sigma}{2} k \left\| \frac{1}{k} \int_{I^i} \mathbf{E}(\tau) d\tau - \mathbf{e}^i \right\|^2 + \frac{\sigma}{2} k \|\nabla(\mathcal{R}_h p - P)^i\|^2 \\
\leq & \frac{\kappa}{8} k \left\| \frac{1}{k} \int_{I^i} \nabla p(\tau) d\tau - \nabla p^i \right\|^2 + \frac{\kappa}{8} k \|\nabla(p - \mathcal{R}_h p)^i\|^2 \\
& + \frac{\kappa}{8} k \|\nabla(\mathcal{R}_h p - P)^i\|^2 + 2\kappa k \|\mathcal{I}_h \mathbf{E}^i - \mathbf{e}^i\|^2 \\
& + \frac{\sigma}{2} k \left\| \frac{1}{k} \int_{I^i} \mathbf{E}(\tau) d\tau - \mathbf{E}^i \right\|^2 + \frac{\sigma}{2} k \|\mathbf{E}^i - \mathcal{I}_h \mathbf{E}^i\|^2 \\
& + \frac{\sigma}{2} k \|\mathcal{I}_h \mathbf{E}^i - \mathbf{e}^i\|^2 + \frac{\kappa}{2} k \|\nabla(\mathcal{R}_h p - P)^i\|^2. \quad (3.23)
\end{aligned}$$

Using the above estimate, the inequality (3.22) can be written as

$$\begin{aligned}
& \epsilon(\Delta^-(\mathcal{I}_h \mathbf{E}^i - \mathbf{e}^i), \mathcal{I}_h \mathbf{E}^i - \mathbf{e}^i) + \mu(\Delta^-(\mathcal{P}_H \mathbf{H}^i - \mathbf{h}^i), \mathcal{P}_H \mathbf{H}^i - \mathbf{h}^i) \\
& + (\Delta^-(c_0 + \mathcal{B})(\mathcal{R}_h p^i - P^i), \mathcal{R}_h p^i - P^i) \\
\leq & \epsilon k(k^{-1} \Delta^-(\mathcal{I}_h \mathbf{E}^i - \mathbf{E}^i), \mathcal{I}_h \mathbf{E}^i - \mathbf{e}^i) - \sigma k \left(\frac{1}{k} \int_{I^i} \mathbf{E}(\tau) d\tau - \mathcal{I}_h \mathbf{E}^i, \mathcal{I}_h \mathbf{E}^i - \mathbf{e}^i \right) \\
& - \frac{\sigma}{2} k (\mathcal{I}_h \mathbf{E}^i - \mathbf{e}^i, \mathcal{I}_h \mathbf{E}^i - \mathbf{e}^i) - k (\mathcal{P}_H \mathbf{H}^i - \mathbf{H}^i, \nabla \times (\mathcal{I}_h \mathbf{E}^i - \mathbf{e}^i)) \\
& - k \left(\mathbf{H}^i - \frac{1}{k} \int_{I^i} \mathbf{H}(\tau) d\tau, \nabla \times (\mathcal{I}_h \mathbf{E}^i - \mathbf{e}^i) \right) + \mu k (k^{-1} \Delta^-(\mathcal{P}_H \mathbf{H}^i - \mathbf{H}^i), \mathcal{P}_H \mathbf{H}^i - \mathbf{h}^i) \\
& + k (\nabla \times (\mathcal{I}_h \mathbf{E}^i - \mathbf{E}^i), \mathcal{P}_H \mathbf{H}^i - \mathbf{h}^i) + k \left(\nabla \times \left(\mathbf{E}^i - \frac{1}{k} \int_{I^i} \mathbf{E}(\tau) d\tau \right), \mathcal{P}_H \mathbf{H}^i - \mathbf{h}^i \right) \\
& + k (k^{-1} \Delta^-(c_0 + \mathcal{B})(\mathcal{R}_h p^i - p^i), \mathcal{R}_h p^i - P^i) - \kappa k \left(\frac{1}{k} \int_{I^i} \nabla p(\tau) d\tau - \nabla \mathcal{R}_h p^i, \nabla (\mathcal{R}_h p - P)^i \right) \\
& - \frac{3}{8} \kappa k (\nabla (\mathcal{R}_h p - P)^i, \nabla (\mathcal{R}_h p - P)^i) + \frac{\kappa}{8} k \left\| \frac{1}{k} \int_{I^i} \nabla p(\tau) d\tau - \nabla p^i \right\|^2 + \frac{\kappa}{8} k \|\nabla (p - \mathcal{R}_h p)^i\|^2 \\
& + \frac{\sigma}{2} k \left\| \frac{1}{k} \int_{I^i} \mathbf{E}(\tau) d\tau - \mathbf{E}^i \right\|^2 + \frac{\sigma}{2} k \|\mathbf{E}^i - \mathcal{I}_h \mathbf{E}^i\|^2 + \frac{\sigma}{2} k \|\mathcal{I}_h \mathbf{E}^i - \mathbf{e}^i\|^2. \tag{3.24}
\end{aligned}$$

Now we analyze the error terms one by one. To estimate the first term (on the right hand side), we use Lemma 3.1 and Lemma 3.2 to obtain

$$\begin{aligned}
\epsilon k (k^{-1} \Delta^-(\mathcal{I}_h \mathbf{E}^i - \mathbf{E}^i), \mathcal{I}_h \mathbf{E}^i - \mathbf{e}^i) & \leq \frac{1}{2} \epsilon k \|k^{-1} \Delta^-(\mathcal{I}_h \mathbf{E}^i - \mathbf{E}^i)\|^2 + \frac{1}{2} \epsilon k \|\mathcal{I}_h \mathbf{E}^i - \mathbf{e}^i\|^2 \\
& \leq \frac{1}{2} \epsilon \int_{I^i} \|(\mathcal{I}_h \mathbf{E} - \mathbf{E})'_t(t)\|^2 dt + \frac{1}{2} \epsilon k \|\mathcal{I}_h \mathbf{E}^i - \mathbf{e}^i\|^2 \\
& \leq C h^{2m} \int_{I^i} \|\mathbf{E}'_t(t)\|_m^2 dt + \frac{1}{2} \epsilon k \|\mathcal{I}_h \mathbf{E}^i - \mathbf{e}^i\|^2. \tag{3.25}
\end{aligned}$$

To estimate the second term, we add and subtract to the left operand of the inner product the same amount \mathbf{E}^i

$$\begin{aligned}
\sigma k \left(\frac{1}{k} \int_{I^i} \mathbf{E}(\tau) d\tau - \mathcal{I}_h \mathbf{E}^i, \mathcal{I}_h \mathbf{E}^i - \mathbf{e}^i \right) & = \sigma k \left(\left(\frac{1}{k} \int_{I^i} \mathbf{E}(\tau) d\tau - \mathbf{E}^i \right) + (\mathbf{E}^i - \mathcal{I}_h \mathbf{E}^i), \mathcal{I}_h \mathbf{E}^i - \mathbf{e}^i \right) \\
& \leq \frac{1}{2} \sigma k^2 \int_{I^i} \|\mathbf{E}'_t(t)\|^2 dt + \frac{1}{2} C k h^{2m} \|\mathbf{E}\|_{m+1}^2 \\
& + \sigma k \|\mathcal{I}_h \mathbf{E}^i - \mathbf{e}^i\|^2. \tag{3.26}
\end{aligned}$$

The third term is simply

$$\frac{\sigma}{2} k (\mathcal{I}_h \mathbf{E}^i - \mathbf{e}^i, \mathcal{I}_h \mathbf{E}^i - \mathbf{e}^i) = \frac{\sigma}{2} k \|\mathcal{I}_h \mathbf{E}^i - \mathbf{e}^i\|^2.$$

For the fourth term, using [25] and the definition of the projection operator \mathcal{P}_H , we have

$$k\left(\mathcal{P}_H\mathbf{H}^i - \mathbf{H}^i, \nabla \times (\mathcal{I}_h\mathbf{E}^i - \mathbf{e}^i)\right) = 0. \quad (3.27)$$

To estimate the fifth term, see [24], using integration by parts while noticing that the boundary condition is $\mathbf{n} \times \mathbf{E} = 0$,

$$\begin{aligned} k\left(\mathbf{H}^i - \frac{1}{k} \int_{I^i} \mathbf{H}(\tau) d\tau, \nabla \times (\mathcal{I}_h\mathbf{E}^i - \mathbf{e}^i)\right) &= k\left(\nabla \times \left(\mathbf{H}^i - \frac{1}{k} \int_{I^i} \mathbf{H}(\tau) d\tau\right), \mathcal{I}_h\mathbf{E}^i - \mathbf{e}^i\right) \\ &\leq \frac{1}{2}k \left\| \nabla \times \left(\mathbf{H}^i - \frac{1}{k} \int_{I^i} \mathbf{H}(\tau) d\tau\right) \right\|^2 + \frac{1}{2}k \|\mathcal{I}_h\mathbf{E}^i - \mathbf{e}^i\|^2 \\ &= \frac{1}{2}k \left\| (\nabla \times \mathbf{H})^i - \frac{1}{k} \int_{I^i} \nabla \times \mathbf{H}(\tau) d\tau \right\|^2 + \frac{1}{2}k \|\mathcal{I}_h\mathbf{E}^i - \mathbf{e}^i\|^2 \\ &\leq \frac{1}{2}k^2 \int_{I^i} \|\nabla \times \mathbf{H}'_t(t)\|^2 dt + \frac{1}{2}k \|\mathcal{I}_h\mathbf{E}^i - \mathbf{e}^i\|^2. \end{aligned} \quad (3.28)$$

The sixth term can be estimated in a similar fashion to the first, except that we now have a projection instead of an interpolation,

$$\begin{aligned} \mu k(k^{-1}\Delta^-(\mathcal{P}_H\mathbf{H}^i - \mathbf{H}^i), \mathcal{P}_H\mathbf{H}^i - \mathbf{h}^i) &\leq \frac{1}{2}\mu k \|k^{-1}\Delta^-(\mathcal{P}_H\mathbf{H}^i - \mathbf{H}^i)\|^2 + \frac{1}{2}\mu k \|\mathcal{P}_H\mathbf{H}^i - \mathbf{h}^i\|^2 \\ &\leq \frac{1}{2}\mu \int_{I^i} \|(\mathcal{P}_H\mathbf{H} - \mathbf{H})'_t(t)\|^2 dt + \frac{1}{2}\mu k \|\mathcal{P}_H\mathbf{H}^i - \mathbf{h}^i\|^2 \\ &\leq Ch^{2m} \int_{I^i} \|\mathbf{H}'_t(t)\|_m^2 dt + \frac{1}{2}\mu k \|\mathcal{I}_h\mathbf{H}^i - \mathbf{h}^i\|^2. \end{aligned} \quad (3.29)$$

To estimate the seventh term, we apply Lemma 3.1

$$\begin{aligned} k(\nabla \times (\mathcal{I}_h\mathbf{E}^i - \mathbf{E}^i), \mathcal{P}_H\mathbf{H}^i - \mathbf{h}^i) &\leq \frac{1}{2}k \|\nabla \times (\mathcal{I}_h\mathbf{E}^i - \mathbf{E}^i)\|^2 + \frac{1}{2}k \|\mathcal{P}_H\mathbf{H}^i - \mathbf{h}^i\|^2 \\ &\leq \frac{1}{2}kh^{2m} \|\nabla \times \mathbf{E}^i\|_{m+1}^2 + \frac{1}{2}k \|\mathcal{P}_H\mathbf{H}^i - \mathbf{h}^i\|^2. \end{aligned} \quad (3.30)$$

The eighth term, can be estimated by

$$\begin{aligned}
k \left(\nabla \times \left(\mathbf{E}^i - \frac{1}{k} \int_{I^i} \mathbf{E}(\tau) d\tau \right), \mathcal{P}_H \mathbf{H}^i - \mathbf{h}^i \right) &\leq \frac{1}{2} k \left\| \nabla \times \left(\mathbf{E}^i - \frac{1}{k} \int_{I^i} \mathbf{E}(\tau) d\tau \right) \right\|^2 \\
&\quad + \frac{1}{2} k \|\mathcal{P}_H \mathbf{H}^i - \mathbf{h}^i\|^2 \\
&\leq \frac{1}{2} k \left\| (\nabla \times \mathbf{E})^i - \frac{1}{k} \int_{I^i} \nabla \times \mathbf{E}(\tau) d\tau \right\|^2 \\
&\quad + \frac{1}{2} k \|\mathcal{P}_H \mathbf{H}^i - \mathbf{h}^i\|^2 \\
&\leq \frac{1}{2} k^2 \int_{I^i} \|\nabla \times \mathbf{E}'_t(t)\|^2 dt + \frac{1}{2} k \|\mathcal{P}_H \mathbf{H}^i - \mathbf{h}^i\|^2.
\end{aligned} \tag{3.31}$$

Since $(c_0 + \mathcal{B})$ is bounded, for the ninth term, we have

$$\begin{aligned}
k(k^{-1} \Delta^-(c_0 + \mathcal{B})(\mathcal{R}_h p^i - p^i), \mathcal{R}_h p^i - P^i) &\leq \frac{1}{2} k \|k^{-1} \Delta^-(c_0 + \mathcal{B})(\mathcal{R}_h p^i - p^i)\|^2 \\
&\quad + \frac{1}{2} k \|\mathcal{R}_h p^i - P^i\|^2 \\
&\leq \frac{1}{2} k^2 \|c_0 + \mathcal{B}\| \int_{I^i} \|(\mathcal{R}_h p - p)'_t(t)\|^2 dt \\
&\quad + \frac{1}{2} k \|\mathcal{R}_h p^i - P^i\|^2.
\end{aligned} \tag{3.32}$$

We evaluate the tenth and eleventh term together, using Young's inequality and then Lemma 3.4 and Lemma 3.7,

$$\begin{aligned}
& - \kappa k \left(\frac{1}{k} \int_{I^i} \nabla p(\tau) d\tau - \nabla \mathcal{R}_h p^i, \nabla(\mathcal{R}_h p - P)^i \right) - \frac{3}{8} \kappa k \left(\nabla(\mathcal{R}_h p - P)^i, \nabla(\mathcal{R}_h p - P)^i \right) \\
&\leq \kappa k \left(\nabla \mathcal{R}_h p^i - \frac{1}{k} \int_{I^i} \nabla p(\tau) d\tau, \nabla \mathcal{R}_h p^i - \frac{1}{k} \int_{I^i} \nabla p(\tau) d\tau \right) + \frac{\kappa}{4} k \left(\nabla(\mathcal{R}_h p - P)^i, \nabla(\mathcal{R}_h p - P)^i \right) \\
&\quad - \frac{3}{8} \kappa k \left(\nabla(\mathcal{R}_h p - P)^i, \nabla(\mathcal{R}_h p - P)^i \right) \\
&= \kappa k \left\| \nabla \mathcal{R}_h p^i - \frac{1}{k} \int_{I^i} \nabla p(\tau) d\tau \right\|^2 - \frac{\kappa}{8} k \|\nabla(\mathcal{R}_h p - P)^i, \nabla(\mathcal{R}_h p - P)^i\|^2 \\
&\leq \kappa k \left\| \nabla \mathcal{R}_h p^i - \frac{1}{k} \int_{I^i} \nabla p(\tau) d\tau \right\|^2 \\
&\leq \kappa k \|\nabla(\mathcal{R}_h p - p)^i\|^2 + \kappa k \left\| \nabla p^i - \frac{1}{k} \int_{I^i} \nabla p(\tau) d\tau \right\|^2 \\
&\leq \kappa k h^{2m} \|p\|_{m+1}^2 + \kappa k^2 \int_{I^i} \|\nabla p'_t(t)\|^2 dt.
\end{aligned} \tag{3.33}$$

The twelfth term is estimated using Lemma 3.4,

$$\frac{\kappa}{8}k \left\| \frac{1}{k} \int_{I^i} \nabla p(\tau) d\tau - \nabla p^i \right\|^2 \leq \frac{1}{8} \kappa k^2 \int_{I^i} \|\nabla p'_t(t)\|^2 dt. \quad (3.34)$$

We obtain that the thirteenth term is 0 from the definition of the projection \mathcal{R}_h ,

$$\frac{\kappa}{8}k \|\nabla(p - \mathcal{R}_h p)^i\|^2 = 0. \quad (3.35)$$

The fourteenth term is also estimated using Lemma 3.4,

$$\frac{\sigma}{2}k \left\| \frac{1}{k} \int_{I^i} \mathbf{E}(\tau) d\tau - \mathbf{E}^i \right\|^2 \leq \frac{\sigma}{2}k^2 \int_{I^i} \|\mathbf{E}'_t(t)\|^2 dt. \quad (3.36)$$

Adding all the above inequalities together and summing both sides of the resulting inequality over $i = 1, 2, \dots, n$, while keeping in mind that for an arbitrary function f ,

$$\sum_{i=1}^n \int_{I^i} f dt = \int_0^{nk} f dt \leq \int_0^T \|f\| dt, \quad (3.37)$$

we have, since \mathcal{B} is both monotone and bounded,

$$\begin{aligned} & \frac{\epsilon}{2} \|\mathcal{I}_h \mathbf{E}^n - \mathbf{e}^n\|^2 + \frac{\mu}{2} \|\mathcal{P}_H \mathbf{H}^n - \mathbf{h}^n\|^2 + \frac{1}{2} c_0 \|\mathcal{R}_h p^n - P^n\|^2 \\ & \frac{\epsilon}{2} \|\mathcal{I}_h \mathbf{E}^n - \mathbf{e}^n\|^2 + \frac{\mu}{2} \|\mathcal{P}_H \mathbf{H}^n - \mathbf{h}^n\|^2 + \frac{1}{2} (c_0 + \mathcal{B}) \|\mathcal{R}_h p^i - P^i\|^2 \\ \leq & \frac{\epsilon}{2} \|\mathcal{I}_h \mathbf{E}^0 - \mathbf{e}^0\|^2 + \frac{\mu}{2} \|\mathcal{P}_H \mathbf{H}^0 - \mathbf{h}^0\|^2 + \frac{1}{2} (c_0 + \mathcal{B}) \|\mathcal{R}_h p^0 - P^0\|^2 \\ & + C_1 k \sum_{i=1}^n (\|\mathcal{I}_h \mathbf{E}^i - \mathbf{e}^i\|^2 + \|\mathcal{P}_H \mathbf{H}^i - \mathbf{h}^i\|^2 + \|\mathcal{R}_h p^i - P^i\|^2) \\ & + Ch^{2m} \int_{I^i} \|\mathbf{E}'_t(t)\|_m^2 dt + \frac{1}{2} \sigma k^2 \int_{I^i} \|\mathbf{E}'_t(t)\|^2 dt + \frac{1}{2} Ckh^{2m} \|\mathbf{E}\|_{m+1}^2 \\ & + \frac{1}{2} k^2 \int_{I^i} \|\nabla \times \mathbf{H}'_t(t)\|^2 dt + Ch^{2m} \int_{I^i} \|\mathbf{H}'_t(t)\|_m^2 dt \\ & + \frac{1}{2} kh^{2m} \|\nabla \times \mathbf{E}^i\|_{m+1}^2 + \frac{1}{2} k^2 \int_{I^i} \|\nabla \times \mathbf{E}'_t(t)\|^2 dt \\ & + \kappa kh^{2m} \|p\|_{m+1}^2 + \kappa k^2 \int_{I^i} \|\nabla p'_t(t)\|^2 dt \\ & + \frac{1}{8} \kappa k^2 \int_{I^i} + \frac{\sigma}{2} k^2 \int_{I^i} \|\mathbf{E}'_t(t)\|^2 dt. \end{aligned} \quad (3.38)$$

Combining terms and using the fact $\mathcal{I}_h \mathbf{E}^0 - \mathbf{e}^0 = 0$, $\mathcal{P}_H \mathbf{H}^0 - \mathbf{h}^0 = 0$, and $\mathcal{R}_h p^0 - P^0 = 0$, due to (3.6), and that $kn \leq T$, we can simply rewrite (3.39) as

$$\begin{aligned} & \epsilon \|\mathcal{I}_h \mathbf{E}^n - \mathbf{e}^n\|^2 + \mu \|\mathcal{P}_H \mathbf{H}^n - \mathbf{h}^n\|^2 + c_0 \|\mathcal{R}_h p^n - P^n\|^2 \\ & \leq C(k^2 + h^{2m}) + C_2 k \sum_{i=1}^n (\|\mathcal{I}_h \mathbf{E}^i - \mathbf{e}^i\|^2 + \|\mathcal{P}_H \mathbf{H}^i - \mathbf{h}^i\|^2 + \|\mathcal{R}_h p^i - P^i\|^2). \end{aligned} \quad (3.40)$$

If we move the n -th terms $\|\mathcal{I}_h \mathbf{E}^n - \mathbf{e}^n\|$ and $\|\mathcal{P}_H \mathbf{H}^n - \mathbf{h}^n\|$ to the left side and adjust the coefficients, we can write

$$\begin{aligned} & \epsilon \|\mathcal{I}_h \mathbf{E}^n - \mathbf{e}^n\|^2 + \mu \|\mathcal{P}_H \mathbf{H}^n - \mathbf{h}^n\|^2 + c_0 \|\mathcal{R}_h p^n - P^n\|^2 \\ & \leq C(k^2 + h^{2m}) + C_3 k \sum_{i=1}^{n-1} (\|\mathcal{I}_h \mathbf{E}^i - \mathbf{e}^i\|^2 + \|\mathcal{P}_H \mathbf{H}^i - \mathbf{h}^i\|^2 + \|\mathcal{R}_h p^i - P^i\|^2). \end{aligned} \quad (3.41)$$

Using the Gronwall's Lemma [36], we obtain

$$\epsilon \|\mathcal{I}_h \mathbf{E}^n - \mathbf{e}^n\|^2 + \mu \|\mathcal{P}_H \mathbf{H}^n - \mathbf{h}^n\|^2 + c_0 \|\mathcal{R}_h p^n - P^n\|^2 \leq C(k^2 + h^{2m}) e^{C_3 nk},$$

and finally

$$\begin{aligned} & \epsilon \|\mathbf{E}^n - \mathbf{e}^n\|^2 + \mu \|\mathbf{H}^n - \mathbf{h}^n\|^2 + c_0 \|p^n - P^n\|^2 \\ & \leq 2\epsilon (\|\mathbf{E}^n - \mathcal{I}_h \mathbf{E}^n\|^2 + \|\mathcal{I}_h \mathbf{E}^n - \mathbf{e}^n\|^2) + 2\mu (\|\mathbf{H}^n - \mathcal{P}_H \mathbf{H}^n\|^2 + \|\mathcal{P}_H \mathbf{H}^n - \mathbf{h}^n\|^2) \\ & \quad + 2c_0 (\|p^n - \mathcal{R}_h p^n\|^2 + \|\mathcal{R}_h p^n - P^n\|^2) \\ & \leq C h^{2m} \|\mathbf{E}^n\|_{m+1}^2 + C h^{2m} \|\mathbf{H}^n\|_m^2 + 2\eta (\|\mathcal{I}_h \mathbf{E}^n - \mathbf{e}^n\|^2 + \|\mathcal{P}_H \mathbf{H}^n - \mathbf{h}^n\|^2) + 2c_0 \|\mathcal{R}_h p^n - P^n\|^2 \\ & \leq C(k^2 + h^{2m}). \end{aligned} \quad (3.42)$$

To obtain the estimate for $\mathbf{u}(t_n) - \mathbf{U}^n$, we define the projection $\mathcal{P}_{\mathbf{u}} : H_0^1(\Omega) \rightarrow \mathbb{V}_h$ for $\mathbf{u} \in H_0^1(\Omega)$

$$a(\mathbf{u} - \mathcal{P}_{\mathbf{u}} \mathbf{u}, \mathbf{v}) = 0, \quad \forall \mathbf{v} \in \mathbb{V}_h.$$

We write the error $\mathbf{u}^n - \mathbf{U}^n$ as

$$\mathbf{u}^n - \mathbf{U}^n = \mathbf{u}^n - \mathcal{P}_{\mathbf{u}} \mathbf{u}^n + \mathcal{P}_{\mathbf{u}} \mathbf{u}^n - \mathbf{U}^n = \delta_{\mathbf{u}}^n + \theta_{\mathbf{u}}^n,$$

where $\delta_{\mathbf{u}}^n = \mathbf{u}^n - \mathcal{P}_{\mathbf{u}} \mathbf{u}^n$ and $\theta_{\mathbf{u}}^n = \mathcal{P}_{\mathbf{u}} \mathbf{u}^n - \mathbf{U}^n$. As in the proof of Lemma 3.8, it is easy to verify that the projection error $\delta_{\mathbf{u}}$ satisfies

$$\|\delta_{\mathbf{u}}\| \leq C(\mathbf{u}) h^m.$$

Subtracting (3.3) from (2.26), we have that

$$a(\theta_{\mathbf{u}}^n, \mathbf{v}) = a(\mathbf{u}^n - \mathbf{U}^n, \mathbf{v}) = -(\nabla(P^n - p^n), \mathbf{v}), \quad \forall \mathbf{v} \in \mathbb{V}_h.$$

Since we know that the bilinear form a is both bounded and coercive, with $\mathbf{v} = \theta_{\mathbf{u}}^n$ in the above equation, there exist a number α and a number C such that

$$\alpha \|\theta_{\mathbf{u}}^n\|_1^2 \leq a(\theta_{\mathbf{u}}^n, \theta_{\mathbf{u}}^n) = -(\nabla(P^n - p^n), \theta_{\mathbf{u}}^n) \leq C \|p^n - P^n\| \|\theta_{\mathbf{u}}^n\|_1,$$

hence

$$\|\theta_{\mathbf{u}}^n\|_1 \leq \frac{C}{\alpha} \|p^n - P^n\| \leq C_1 \|l_0 - l\| + C_2 (h^m + k).$$

□

Chapter 4

Numerical example

We now illustrate the theory described above. To that end, we construct solutions and use the proposed method to approximate this solution. Let $\Omega = [-1, 1] \times [-1, 1] \times [-1, 1]$, $I = [0, 1]$. Set $\epsilon = 1$, $\sigma = 2$, $\mu = 1$, $\lambda_c = 2$, $G = 1$, $\alpha = 1$, $c_0 = 1$, $\kappa = 2$, $L = 1$. The solution is given by

$$\mathbf{E} = (\sin(\pi x) \sin(\pi y) \sin(\pi z), \sin(\pi x) \sin(\pi y) \sin(\pi z), \sin(\pi x) \sin(\pi y) \sin(\pi z))(t^2 + 1),$$

$$\mathbf{H} = - (\sin(\pi x) \cos(\pi y) \sin(\pi z) - \sin(\pi x) \sin(\pi y) \cos(\pi z),$$

$$\sin(\pi x) \sin(\pi y) \cos(\pi z) - \cos(\pi x) \sin(\pi y) \sin(\pi z),$$

$$\cos(\pi x) \sin(\pi y) \sin(\pi z) - \sin(\pi x) \cos(\pi y) \sin(\pi z))\pi\left(\frac{t^3}{3} + t\right)$$

$$\mathbf{u} = (\sin(\pi x) \sin(\pi y) \sin(\pi z), 0, 0)(t^2 + 1),$$

and

$$p = \sin(\pi x) \sin(\pi y) \sin(\pi z)(t^2 + 1).$$

Note that the system of equations is not homogeneous if we use this set of solutions. The right hand side is now $(\mathbf{J}, 0, \mathbf{f}, g)^T$, where

$$\begin{aligned} \mathbf{J}^T = & \begin{pmatrix} \sin(\pi x) \sin(\pi y) \sin(\pi z) \\ \sin(\pi x) \sin(\pi y) \sin(\pi z) \\ \sin(\pi x) \sin(\pi y) \sin(\pi z) \end{pmatrix} 2 \left(\frac{\pi^2}{3} t^3 + t^2 + (\pi^2 + 1)t + 1 \right) \\ & + \begin{pmatrix} \cos(\pi x) \cos(\pi y) \sin(\pi z) + \cos(\pi x) \sin(\pi y) \cos(\pi z) \\ \sin(\pi x) \cos(\pi y) \cos(\pi z) + \cos(\pi x) \cos(\pi y) \sin(\pi z) \\ \cos(\pi x) \sin(\pi y) \cos(\pi z) + \sin(\pi x) \cos(\pi y) \cos(\pi z) \end{pmatrix} \pi^2 \left(\frac{t^3}{3} + t \right) \\ & - \begin{pmatrix} \cos(\pi x) \sin(\pi y) \sin(\pi z) \\ \sin(\pi x) \cos(\pi y) \sin(\pi z) \\ \sin(\pi x) \sin(\pi y) \cos(\pi z) \end{pmatrix} \pi(t^2 + 1) \end{aligned}$$

$$\begin{aligned} \mathbf{f} = & (5\pi^2 \sin(\pi x) \sin(\pi y) \sin(\pi z), -2\pi^2 \cos(\pi x) \cos(\pi y) \sin(\pi z)(t^2 + 1), \\ & -2\pi^2 \cos(\pi x) \sin(\pi y) \cos(\pi z)), \end{aligned}$$

and

$$\begin{aligned} g = & ((\sin(\pi x) + \pi \cos(\pi x))2t + \sin(\pi x)6\pi^2(t^2 + 1)) \sin(\pi y) \sin(\pi z) \\ & + (\cos(\pi x) \sin(\pi y) \sin(\pi z) + \sin(\pi x) \cos(\pi y) \sin(\pi z) + \sin(\pi x) \sin(\pi y) \cos(\pi z))\pi(t^2 + 1). \end{aligned}$$

One can check that the boundary conditions are satisfied

$$\mathbf{E} \times \mathbf{n} = \mathbf{0}, \quad \text{on } \partial\Omega, \quad (4.1)$$

$$\mathbf{u} = \mathbf{0}, p = 0, \quad \text{on } \partial\Omega. \quad (4.2)$$

The tables below provide some information about the discretizations used (time step k , mesh parameter h , number of elements, and number of degrees of freedom/unknowns) as

well as the observed relative errors and convergence rates. The observed convergence rates were computed from the observed errors which were measured using the L^2 -norm. These observed rates are in good agreement with the theory.

Table 1 shows the relative errors for each variable and the corresponding convergence rates when using order 1 Nédélec edge element $N1_1^e$ and linear Lagrange element. (r.e. is the relative error)

k	h	DOFs	r.e. \mathbf{E}	rate	r.e. \mathbf{H}	rate	r.e. \mathbf{u}	rate	r.e. p	rate
1/10	1/3	913	0.6225	-	0.4172	-	0.4037	-	0.4010	-
1/20	1/6	6034	0.3427	0.86	0.2130	0.97	0.1249	1.69	0.1182	1.76
1/40	1/12	4.4×10^4	0.1757	0.96	0.1070	0.99	0.0339	1.88	0.0309	1.94
1/80	1/24	3.3×10^5	0.0885	0.99	0.0535	1.00	0.0087	1.96	0.0078	1.99

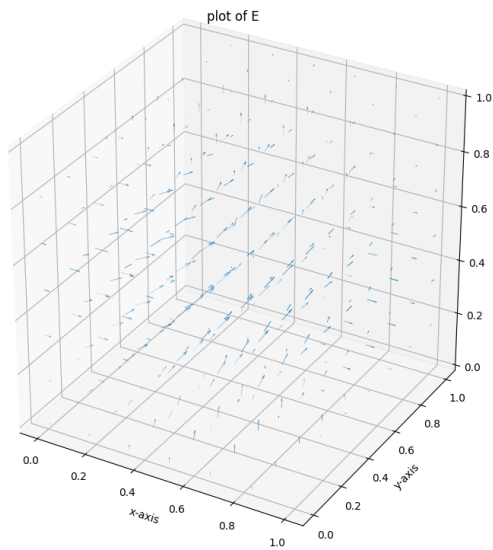
Table 4.1: A nice table

Table 2 shows the relative errors for each variable and the corresponding convergence rates when we using order 2 Nédélec edge element $N1_2^e$ and quadratic Lagrange element.

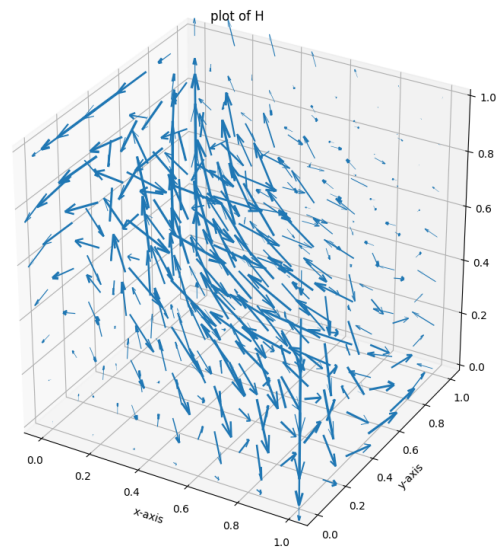
k	h	DOFs	r.e. \mathbf{E}	rate	r.e. \mathbf{H}	rate	r.e. \mathbf{u}	rate	r.e. p	rate
1/10	1/3	4306	0.1620	-	0.0747	-	0.04749	-	0.04569	-
1/40	1/6	3.0×10^4	0.0438	1.89	0.0192	1.96	0.005307	3.16	0.005044	3.18
1/160	1/12	2.3×10^5	0.0113	1.96	0.0048	1.99	6.1×10^{-4}	3.12	6.0×10^{-4}	3.08
1/640	1/24	1.8×10^6	0.0028	1.99	0.0012	2.00	7.4×10^{-5}	3.04	7.7×10^{-5}	2.95

Table 4.2: Relative L^2 -norm errors and convergence rates using order 2 Lagrange elements and Nédélec elements.

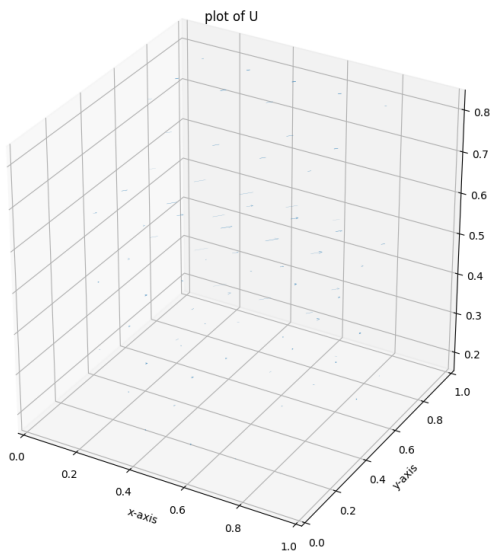
We plot the approximate solutions.



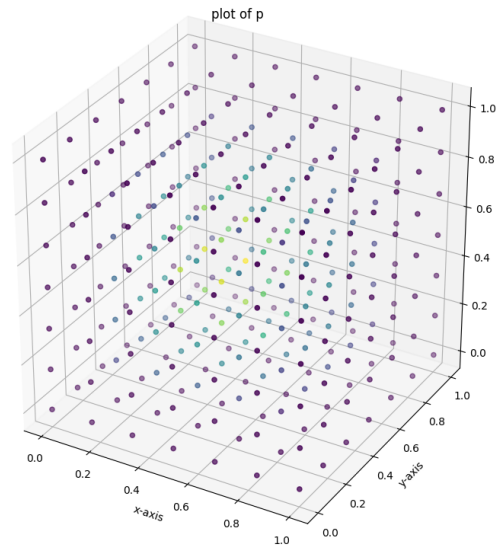
(a) Electric field \mathbf{E}



(b) Magnetic field \mathbf{H}



(c) Solid displacement \mathbf{u}



(d) Pressure p

Figure 4.1: Plot of four variables \mathbf{E} , \mathbf{H} , \mathbf{u} , p .

A set of solutions which satisfy the homogeneous equations (2.19) – (2.22) with the initial condition

$$\mathbf{E}_0 = (\sin(\pi y) \sin(\pi z), \sin(\pi z) \sin(\pi x), \sin(\pi x) \sin(\pi y)), \quad (4.3)$$

$$\begin{aligned} \mathbf{H}_0 = & (\pi \sin(\pi x)(\cos(\pi y) - \cos(\pi z)), \pi \sin(\pi y)(\cos(\pi z) - \cos(\pi x)), \\ & \pi \sin(\pi z)(\cos(\pi x) - \cos(\pi y))), \end{aligned} \quad (4.4)$$

$$\mathbf{u}_0 = (3 \sin(\pi x) \sin(\pi y) \sin(\pi z), 3 \sin(\pi x) \sin(\pi y) \sin(\pi z), 0), \quad (4.5)$$

$$p_0 = (\sin(\pi x) \sin(\pi y) \sin(\pi z)), \quad (4.6)$$

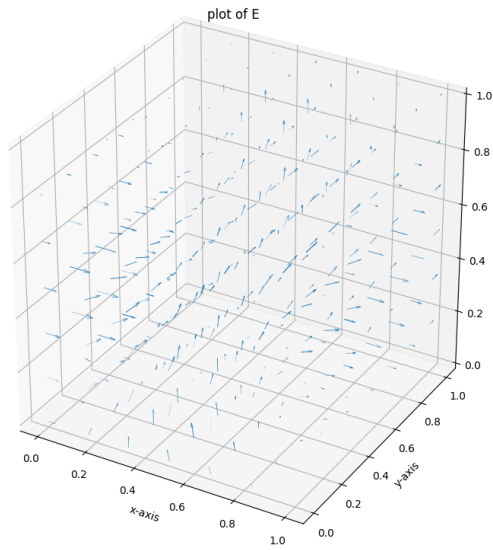
is

To better illustrate the effect of the coupling parameter L , we calculated solutions of the equations for two values of L while keeping other parameters fixed. For comparison we plot these solution below. We applied the boundary conditions as

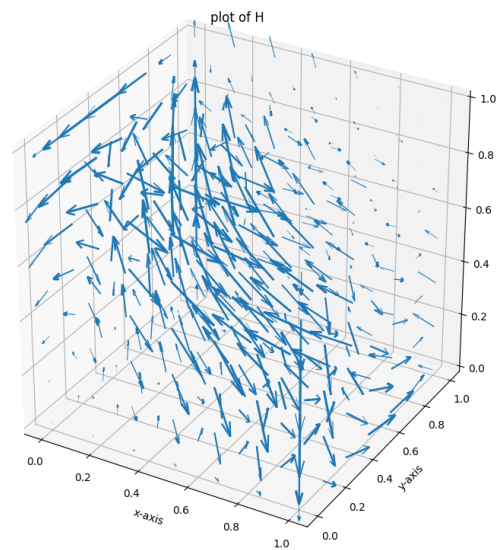
$$\begin{pmatrix} \mathbf{E} \\ \mathbf{H} \\ \mathbf{u} \\ p \end{pmatrix} = \begin{pmatrix} 0, & 0, & 0 \\ 0, & 0, & 0 \\ 0, & 0, & x \\ 0 \end{pmatrix}$$

and initial conditions as

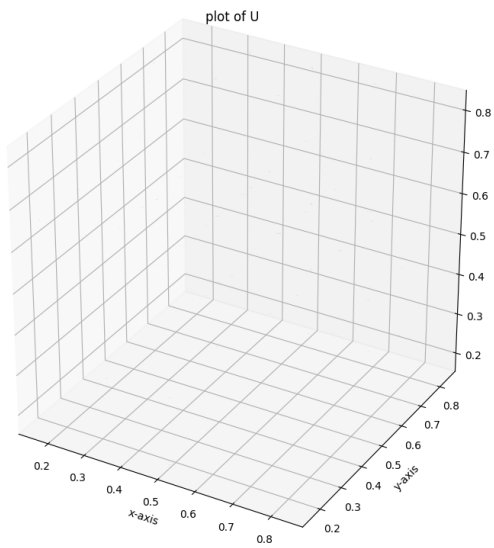
$$\begin{pmatrix} \mathbf{E} \\ \mathbf{H} \\ \mathbf{u} \\ p \end{pmatrix} = \begin{pmatrix} 30xy(1-y)z(1-z), & 30yz(1-z)x(1-x), & 30zx(1-x)y(1-y) \\ 30(x-1)x(y-z), & 30(y-1)y(z-x), & 30(z-1)z(x-y) \\ \sin(\pi x) \sin(\pi y) \sin(\pi z), & 0, & x \\ 10 \sin(\pi x) \sin(\pi y) \sin(\pi z) \end{pmatrix}.$$



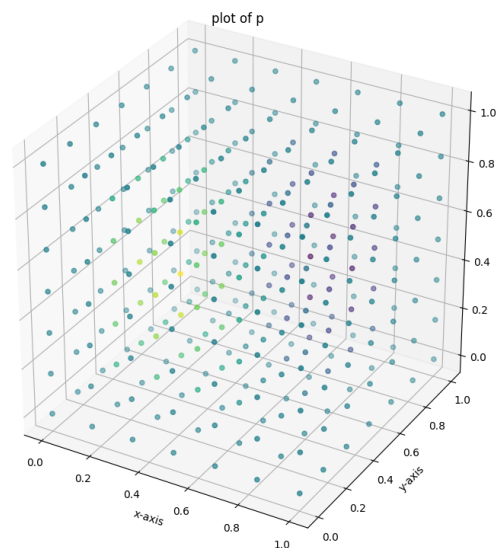
(a) Plot of \mathbf{E}



(b) Plot of \mathbf{H}

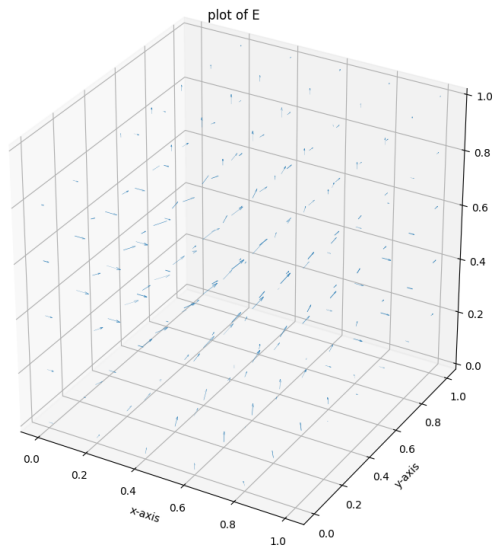


(c) Plot of u

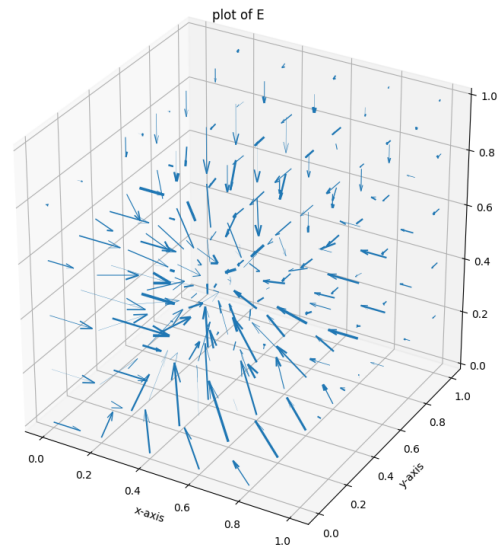


(d) Plot of p

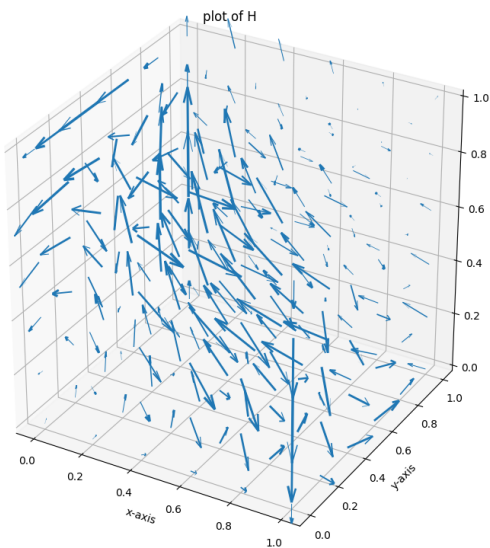
Figure 4.2: Plot of four variables \mathbf{E} , \mathbf{H} , u , p



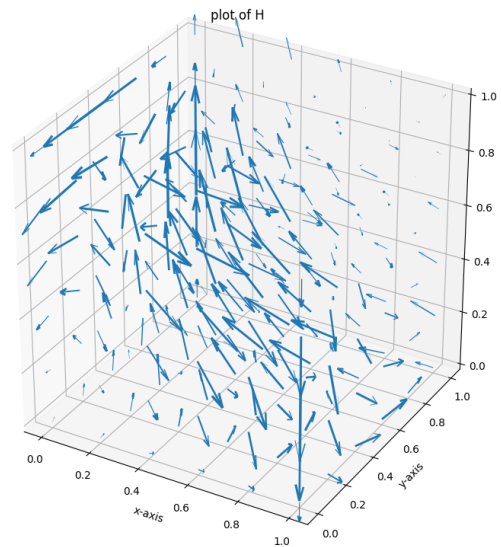
(a) Electric field \mathbf{E} when $L = 0$



(b) Electric field \mathbf{E} when $L = 0.3$

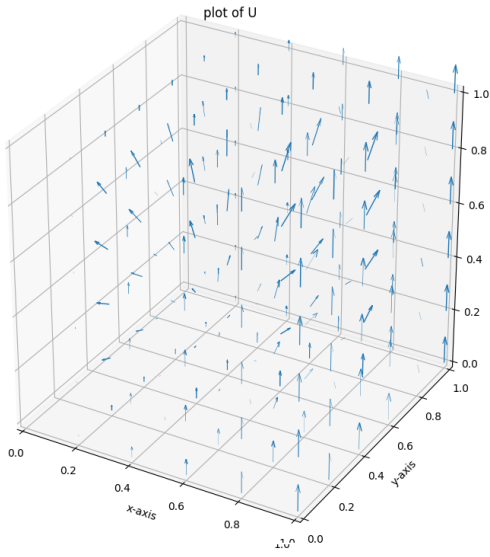


(c) Magnetic field \mathbf{H} when $L = 0$

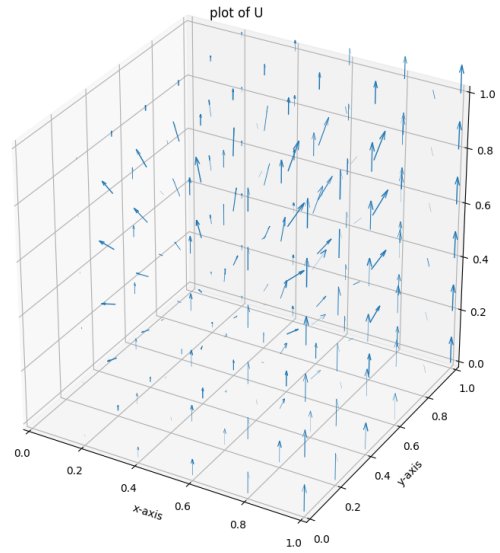


(d) Magnetic field \mathbf{H} when $L = 0.3$

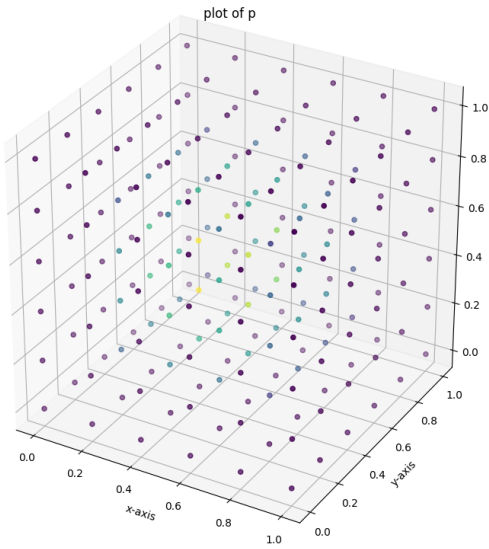
Figure 4.3: Plot of electromagnetic fields \mathbf{E} and \mathbf{H}



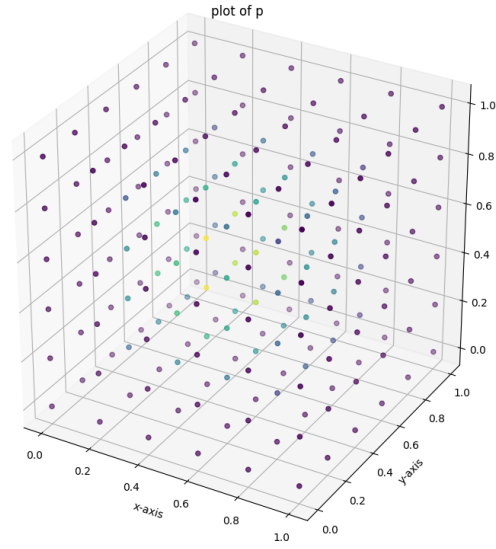
(a) Solid displacement \mathbf{u} when $L = 0$



(b) Solid displacement \mathbf{u} when $L = 0.3$



(c) Pressure p when $L = 0$



(d) Pressure p when $L = 0.3$

Figure 4.4: Plot of poroelasticity variables \mathbf{u} and p

Chapter 5

Computation and computer implementation

We implement the numerical scheme using FEniCS [1]. FEniCS is a popular open-source computing platform for solving partial differential equations. FEniCS enables users to quickly translate scientific models into efficient finite element code. With the high-level Python and C++ interfaces to FEniCS, it is easy to get started, but FEniCS offers also powerful capabilities for more experienced programmers. FEniCS runs on a multitude of platforms ranging from laptops to high-performance clusters.

Our FEniCS code is

```
# Poro-electro-elasticity Equations
# epsilon dE/dt + sigma E - curl H - L grad p = J
# mu dH/dt + curl E = 0
# -lambda grad div u - G div grad u + alpha p = f
# d/dt(c p + alpha div u) + L div E - kappa laplacian p = g

from fenics import *
from ufl import nabla_div
import numpy as np
import matplotlib.pyplot as plt

# Definition of constants and parameters
epsilon0 = 1
sigma0 = 2*pi*pi
L0 = 0.5
mu0 = 1
lambda0 = 2
G0 = 1
alpha0 = 1
```

```

c0 = 1
kappa0 = 1/(3*pi*pi)

T = 1.0 # final time
num_steps = 10 # number of time steps
dt = T/ num_steps # time step size

# Create mesh and define function space
# Load mesh
mesh = UnitCubeMesh(10, 10, 10)

# Build function space
D1 = FiniteElement("N1curl", mesh.ufl_cell(), 1)
B1 = FiniteElement("RT", mesh.ufl_cell(), 1)
V = VectorElement("Lagrange", mesh.ufl_cell(), 1)
Q = FiniteElement("Lagrange", mesh.ufl_cell(), 1)
element = MixedElement([D1, B1, V, Q])
W = FunctionSpace(mesh, element)

# Exact solutions, boundary conditions and known functions
E_ex = Expression(('sin(pi*x[1])*sin(pi*x[2])*exp(-t)', \
    'sin(pi*x[2])*sin(pi*x[0])*exp(-t)', \
    'sin(pi*x[0])*sin(pi*x[1])*exp(-t)'), degree = 2, t = 0)
H_ex = Expression(('pi*sin(pi*x[0])*(cos(pi*x[1])-cos(pi*x[2]))*exp(-t)', \
    'pi*sin(pi*x[1])*(cos(pi*x[2])-cos(pi*x[0]))*exp(-t)', \
    'pi*sin(pi*x[2])*(cos(pi*x[0])-cos(pi*x[1]))*exp(-t)'), degree = 2, t = 0)
u_D = Expression(('sin(pi*x[0])*sin(pi*x[1])*sin(pi*x[2])*exp(-t)', '0', '0'), degree
= 2, t = 0)
p_D = Expression('sin(pi*x[0])*sin(pi*x[1])*sin(pi*x[2])*exp(-t)', degree = 2, t
= 0)

J = Expression(('(-1-0.5*pi*cos(pi*x[0]))*sin(pi*x[1])*sin(pi*x[2])*exp(-t)',
    '(-1-0.5*pi*cos(pi*x[1]))*sin(pi*x[2])*sin(pi*x[0])*exp(-t)', \
    '(-1-0.5*pi*cos(pi*x[2]))*sin(pi*x[0])*sin(pi*x[1])*exp(-t)'), \

```

```

    degree = 2, t = 0)
f = Expression(('5*pi*pi*sin(pi*x[0])*sin(pi*x[1])*sin(pi*x[2])*exp(-t)
+ pi*cos(pi*x[0])*sin(pi*x[1])*sin(pi*x[2])*exp(-t)',
'-2*pi*pi*cos(pi*x[0])*cos(pi*x[1])*sin(pi*x[2])*exp(-t)
+ pi*cos(pi*x[1])*sin(pi*x[2])*sin(pi*x[0])*exp(-t)',
'-2*pi*pi*cos(pi*x[0])*sin(pi*x[1])*cos(pi*x[2])*exp(-t)
+ pi*cos(pi*x[2])*sin(pi*x[0])*sin(pi*x[1])*exp(-t)'),
    degree = 2, t = 0)
g = Expression('-pi*cos(pi*x[0])*sin(pi*x[1])*sin(pi*x[2])*exp(-t)', \
    degree = 2, t = 0)
U_0 = Expression(('sin(pi*x[1])*sin(pi*x[2])', 'sin(pi*x[2])*sin(pi*x[0])',
'sin(pi*x[0])*sin(pi*x[1])',
'pi*sin(pi*x[0])*(cos(pi*x[1])-cos(pi*x[2]))',
'pi*sin(pi*x[1])*(cos(pi*x[2])-cos(pi*x[0]))',
'pi*sin(pi*x[2])*(cos(pi*x[0])-cos(pi*x[1]))', \
'sin(pi*x[0])*sin(pi*x[1])*sin(pi*x[2])', '0', '0', \
'sin(pi*x[0])*sin(pi*x[1])*sin(pi*x[2])'), degree = 2)
tol = 1E-14

def boundary(x, on_boundary):
    return on_boundary

bcD = DirichletBC(W.sub(0), Constant((0.0, 0.0, 0.0)), DomainBoundary())
bcB = DirichletBC(W.sub(1), Constant((0.0, 0.0, 0.0)), DomainBoundary())
bcu = DirichletBC(W.sub(2), Constant((0.0, 0.0, 0.0)), DomainBoundary())
bcp = DirichletBC(W.sub(3), Constant(0.0), boundary)
bc = [bcD, bcB, bcu, bcp]

# Define expressions used in variational forms
dt = Constant(dt)
epsilon0 = Constant(epsilon0)
sigma0 = Constant(sigma0)
L0 = Constant(L0)
mu0 = Constant(mu0)

```

```

lambda0 = Constant(lambda0)
G0 = Constant(G0)
alpha0 = Constant(alpha0)
c0 = Constant(c0)
kappa0 = Constant(kappa0)

# Define initial value
bfU_n = project(U_0, W)
# solutions got from last time step
E_n, H_n, bfu_n, p_n = split(bfU_n)

# Define variational problem
E, H, bfu, p = TrialFunctions(W)
D, B, bfv, q = TestFunctions(W)

# bilinear form
a = epsilon0*inner(E, D)*dx + dt*sigma0*inner(E, D)*dx - dt*inner(H, curl(D))*dx\
    - dt*L0*inner(nabla_grad(p), D)*dx + mu0*inner(H, B)*dx + dt*inner(curl(E), B)*dx\
    + lambda0*inner(nabla_div(bfu), nabla_div(bfv))*dx\
    + G0*inner(nabla_grad(bfu), nabla_grad(bfv))*dx\
    + c0*inner(p, q)*dx + alpha0*inner(nabla_div(bfu), q)*dx
    - alpha0*inner(p, nabla_div(bfv))*dx\
    - dt*L0*inner(E, nabla_grad(q))*dx + dt*kappa0*inner(nabla_grad(p)
    , nabla_grad(q))*dx\
L = dt*inner(J, D)*dx + epsilon0*inner(E_n, D)*dx + mu0*inner(H_n, B)*dx\
    + inner(f, bfv)*dx + inner((c0*p_n + dt*g), q)*dx\
    + alpha0*inner(nabla_div(bfu_n), q)*dx

# Time-stepping #
bfU = Function(W)
t = 0

for nn in range(num_steps):
    # Update current time
    t += T/ num_steps

```

```

E_ex.t = t
H_ex.t = t
J.t = t
u_D.t = t
p_D.t = t
f.t = t
g.t = t
# Solve variational problem
solve(a == L, bfU, bc)
# Calculate errors
Eh, Hh, Uh, ph = bfU.split()
error_L21 = errornorm(E_ex, Eh, norm_type = 'l2')
error_L22 = errornorm(H_ex, Hh, norm_type = 'l2')
error_L23 = errornorm(u_D, Uh, norm_type = 'l2')
error_L24 = errornorm(p_D, ph, norm_type = 'l2')
ENorm = sqrt(assemble(inner(E_ex, E_ex)*dx(mesh)))
HNorm = sqrt(assemble(inner(H_ex, H_ex)*dx(mesh)))
UNorm = sqrt(assemble(inner(u_D, u_D)*dx(mesh)))
pNorm = sqrt(assemble(inner(p_D, p_D)*dx(mesh)))
rel_err_21 = error_L21/ENorm
rel_err_22 = error_L22/HNorm
rel_err_23 = error_L23/UNorm
rel_err_24 = error_L24/pNorm
print('At t = ', t)
print('relative error ||E - E_ex||/||E|| = ', rel_err_21)
print('relative error ||H - H_ex||/||H|| = ', rel_err_22)
print('relative error ||U - U_ex||/||U|| = ', rel_err_23)
print('relative error ||p - p_ex||/||p|| = ', rel_err_24)
# Update previous solution
bfU.n.assign(bfU)

```

We shall now dissect our FEniCS program in detail.

```

from fenics import *
from ufl import nabla_div

```

```
import numpy as np
import matplotlib.pyplot as plt
```

The first line in the program imports the key classes `UnitSquareMesh`, `FunctionSpace`, `Function`, and so forth, from the FEniCS library. All FEniCS programs for solving PDEs by the finite element method normally start with this line. The second line imports the operation of matrix divergence. NumPy is the fundamental package for scientific computing with Python and Matplotlib is a comprehensive library for creating static, animated, and interactive visualizations in Python.

```
# Create mesh and define function space
# Load mesh
mesh = UnitCubeMesh(10, 10, 10)
```

This sets the domain Ω as a unit cube, and create a mesh on it. There are totally $10 \times 10 \times 10$ uniformly distributed nodes.

```
# Build function space
D1 = FiniteElement("N1curl", mesh.ufl_cell(), 1)
B1 = FiniteElement("RT", mesh.ufl_cell(), 1)
V = VectorElement("Lagrange", mesh.ufl_cell(), 1)
Q = FiniteElement("Lagrange", mesh.ufl_cell(), 1)
element = MixedElement([D1, B1, V, Q])
W = FunctionSpace(mesh, element)
```

The third argument “1” specifies the degree of the finite element. We have used Nedéléc element of order 1 (P_1 in the $\mathcal{P}_r^- \Lambda^k$ family), Raviart-Thomas element of order 1 ($N1_1^f$ in the $\mathcal{P}_r^- \Lambda^k$ family), and linear Lagrange elements for the test functions in the first, second, third and fourth equations, respectively. W is the mixed element function space, each vector in W can be divided into four parts which corresponds to $D1$, $B1$, V and Q , using `split` command. The function space can also be divided, as we will see later.

```
# Exact solutions, boundary conditions and known functions
E_ex = Expression(('sin(pi*x[1])*sin(pi*x[2])*exp(-t)', \
    'sin(pi*x[2])*sin(pi*x[0])*exp(-t)', \
    'sin(pi*x[0])*sin(pi*x[1])*exp(-t)'), degree = 2, t = 0)
```

This is a way to define functions in FEniCS, the argument `degree` is a parameter that specifies how the expression should be treated in computations. On each local element, FEniCS will interpolate the expression into a finite element space of the specified degree. `t=0` is a typical way to treat the time in FEniCS, that is, first declare time as a parameter and initialize it to zero, then update its value in the time loop.

```
def boundary(x, on_boundary):
    return on_boundary
```

The argument `on_boundary` is `True` if x is on the physical boundary of the mesh, so in the present case, where we are supposed to return `True` for all points on the boundary, we can just return the supplied value of `on_boundary`.

```
bcD = DirichletBC(W.sub(0), Constant((0.0, 0.0, 0.0)), DomainBoundary())
bcB = DirichletBC(W.sub(1), Constant((0.0, 0.0, 0.0)), DomainBoundary())
bcu = DirichletBC(W.sub(2), Constant((0.0, 0.0, 0.0)), DomainBoundary())
bcp = DirichletBC(W.sub(3), Constant(0.0), boundary)
bc = [bcD, bcB, bcu, bcp]
```

Our boundary conditions are $\mathbf{n} \times \mathbf{E} = 0$, $\mathbf{u} = 0$ and $p = 0$ on the boundary. `W.sub(i)` corresponds to the i th subspace of W . Boundary conditions for each equation are specified by calling corresponding W 's subspaces. Then, as we constructed the big space W for the four spaces, we declare a vector of boundary conditions, call it `bc`.

```
# Define expressions used in variational forms
dt = Constant(dt)
```

Declare `dt` as a `Constant` object to use it later in declaring bilinear and linear forms.

```
# Define initial value
bfU_n = project(U_0, W)
# solutions got from last time step
E_n, H_n, bfu_n, p_n = split(bfU_n)
```

Here, `bfU = (E, H, bfu, p)` is the unknown vector used in solving the big linear system. Variables with subscript `n` denote the solution obtained from the last step. In each step, `bfU` is recalculated and then its value is passed to `bfU_n` as in the next step, the solution in the last step. `bfU_n` is divided to calculate

errors.

```
# Define variational problem
E, H, bfu, p = TrialFunctions(W)
D, B, bfv, q = TestFunctions(W)
```

We can directly do this because FEniCS knows that W is comprised of four parts, and the order of the spaces is preserved as in the command `element = MixedElement([D1, B1, V, Q])`.

```
# bilinear form
a = epsilon0*inner(E, D)*dx + dt*sigma0*inner(E, D)*dx - dt*inner(H, curl(D))*dx\
  - dt*L0*inner(nabla_grad(p), D)*dx + mu0*inner(H, B)*dx\
  + dt*inner(curl(E), B)*dx\
  + lambda0*inner(nabla_div(bfu), nabla_div(bfv))*dx\
  + G0*inner(nabla_grad(bfu), nabla_grad(bfv))*dx\
  + c0*inner(p, q)*dx + alpha0*inner(nabla_div(bfu), q)*dx\
  - alpha0*inner(p, nabla_div(bfv))*dx\
  - dt*L0*inner(E, nabla_grad(q))*dx + dt*kappa0*inner(nabla_grad(p),\
  nabla_grad(q))*dx\
L = dt*inner(J, D)*dx + epsilon0*inner(E_n, D)*dx + mu0*inner(H_n, B)*dx\
  + inner(f, bfv)*dx + inner((c0*p_n + dt*g), q)*dx\
  + alpha0*inner(nabla_div(bfu_n), q)*dx
```

Here we can see one of the great features of FEniCS. The declaration of the bilinear forms and linear forms are very similar to mathematical formula written in a text file. People with no experience with FEniCS can certainly read these commands. The command `nabla_grad` can be used to calculate the gradient for both a scalar and a vector.

```
for nn in range(num_steps):
    # Update current time
    t += T/ num_steps
    E.ex.t = t
    H.ex.t = t
    J.t = t
    u.D.t = t
```

```
p.D.t = t
```

```
f.t = t
```

```
g.t = t
```

Here we update the time of each function.

```
# Solve variational problem
```

```
solve(a == L, bfU, bc)
```

Here we can see another great feature of FEniCS. We can use `a` to include all bilinear forms and `L` to include all linear forms. Then, simply calls `solve(a == L, bfU, bc)` will ask FEniCS to calculate the solution after applying `bc`) and store it in `bfU`. FEniCS knows which space each function belongs to and will automatically assemble linear systems and solve.

Bibliography

- [1] *www.thefenicsproject.org*.
- [2] M. Biot. Theory of elastic waves in a fluid-saturated porous solid. 1. low frequency range. *J. Acoust. Soc. Am.*, 28:168–178, 1956.
- [3] M. A. Biot. General theory of three-dimensional consolidation. *Journal of applied physics*, 12(2):155–164, 1941.
- [4] M. A. Biot. Theory of propagation of elastic waves in a fluid-saturated porous solid. ii. higher frequency range. *The Journal of the acoustical Society of america*, 28(2):179–191, 1956.
- [5] M. A. Biot. Science and the engineer. *Engineering and Science*, 26(4):30–36, 1963.
- [6] P. B. Bochev and M. D. Gunzburger. *Least-squares finite element methods*, volume 166. Springer Science & Business Media, 2009.
- [7] K. E. Butler, R. D. Russell, A. W. Kepic, and M. Maxwell. Measurement of the seismoelectric response from a shallow boundary. *Geophysics*, 61(6):1769–1778, 1996.
- [8] Y. Cao, S. Chen, and A. Meir. Analysis and numerical approximations of equations of nonlinear poroelasticity. *Discrete & Continuous Dynamical Systems-Series B*, 18(5), 2013.
- [9] A. Cheng. Poroelasticity (theory and applications of transport in porous media), vol. 27, 2016.
- [10] D. Colton. Re showalter, hilbert space methods for partial differential equations (pitman, 1977), xii+196 pp.,£ 1400. *Proceedings of the Edinburgh Mathematical Society*, 22(1):66–66, 1979.
- [11] L. da Vinci. *Codex leicester*. 1506-1510.
- [12] J. Frenkel. On the theory of seismic and seismoelectric phenomena in a moist soil: *Journal of physics ussr*. 1944.
- [13] D. J. Griffiths. Reed college.(1999). introduction to electrodynamics (vol. 3).
- [14] M. W. Haartsen. Coupled electromagnetic and acoustic wavefield modeling in poro-elastic media and its applications in geophysical exploration. 1996.

- [15] S. S. Haines and S. R. Pride. Seismoelectric numerical modeling on a grid. *Geophysics*, 71(6):N57–N65, 2006.
- [16] A. Ivanov. Effect of electrization of earth layers by elastic waves passing through them. *Doklady Akademii Nauk SSSR*, 24(1):42–45, 1939.
- [17] J. Li. Error analysis of fully discrete mixed finite element schemes for 3-d maxwell’s equations in dispersive media. *Computer Methods in Applied Mechanics and Engineering*, 196(33-34):3081–3094, 2007.
- [18] J. Li and Y. Chen. Analysis of a time-domain finite element method for 3-d maxwell’s equations in dispersive media. *Computer methods in applied mechanics and engineering*, 195(33-36):4220–4229, 2006.
- [19] J. L. Lions. Quelques méthodes de résolution des problemes aux limites non linéaires. 1969.
- [20] J. L. Lions and G. Duvaut. *Inequalities in mechanics and physics*. Springer, 1976.
- [21] A. Logg, K.-A. Mardal, G. N. Wells, et al. *Automated Solution of Differential Equations by the Finite Element Method*. Springer, 2012.
- [22] S. R. Mahmoud. Wave propagation in cylindrical poroelastic dry bones. 2010.
- [23] P. Monk. An analysis of nedelec’s method for the spatial discretization of maxwell’s equations. *Journal of Computational and Applied Mathematics*, 47(1):101–121, 1993.
- [24] P. Monk et al. *Finite element methods for Maxwell’s equations*. Oxford University Press, 2003.
- [25] P. B. Monk. A mixed method for approximating maxwell’s equations. *SIAM Journal on Numerical Analysis*, 28(6):1610–1634, 1991.
- [26] J.-C. Nédélec. Mixed finite elements in r3. *Numerische Mathematik*, 35(3):315–341, 1980.
- [27] J. Neev and F. Yeatts. Electrokinetic effects in fluid-saturated poroelastic media. *Physical Review B*, 40(13):9135, 1989.
- [28] M. Oka, T. Noguchi, P. Kumar, K. Ikeuchi, T. Yamamuro, S. Hyon, and Y. Ikada. Development of an artificial articular cartilage. *Clinical materials*, 6(4):361–381, 1990.

- [29] M. Oka, K. Ushio, P. Kumar, K. Ikeuchi, S. Hyon, T. Nakamura, and H. Fujita. Development of artificial articular cartilage. *Proceedings of the Institution of Mechanical Engineers, Part H: Journal of Engineering in Medicine*, 214(1):59–68, 2000.
- [30] D. B. Pengra, S. Xi Li, and P.-z. Wong. Determination of rock properties by low-frequency ac electrokinetics. *Journal of Geophysical Research: Solid Earth*, 104(B12):29485–29508, 1999.
- [31] P. R. Perriñez, F. E. Kennedy, E. E. Van Houten, J. B. Weaver, and K. D. Paulsen. Magnetic resonance poroelastography: an algorithm for estimating the mechanical properties of fluid-saturated soft tissues. *IEEE transactions on medical imaging*, 29(3):746–755, 2010.
- [32] P. R. Perriñez, A. J. Pattison, F. E. Kennedy, J. B. Weaver, and K. D. Paulsen. Contrast detection in fluid-saturated media with magnetic resonance poroelastography. *Medical physics*, 37(7Part1):3518–3526, 2010.
- [33] P. J. Phillips. *Finite element methods in linear poroelasticity: Theoretical and computational results*. PhD thesis, 2005.
- [34] S. Pride. Governing equations for the coupled electromagnetics and acoustics of porous media. *Physical Review B*, 50(21):15678, 1994.
- [35] S. R. Pride, A. F. Gangi, and F. D. Morgan. Deriving the equations of motion for porous isotropic media. *The Journal of the Acoustical Society of America*, 92(6):3278–3290, 1992.
- [36] A. Quarteroni and A. Valli. *Numerical approximation of partial differential equations*, volume 23. Springer Science & Business Media, 2008.
- [37] J. E. Santos. Elastic wave propagation in fluid-saturated porous media. part i. the existence and uniqueness theorems. *ESAIM: Mathematical Modelling and Numerical Analysis*, 20(1):113–128, 1986.
- [38] J. E. Santos, F. I. Zyserman, and P. M. Gauzellino. Numerical electroseismic modeling: a finite element approach. *Applied Mathematics and Computation*, 218(11):6351–6374, 2012.
- [39] R. E. Showalter. Diffusion in poro-elastic media. *Journal of mathematical analysis and applications*, 251(1):310–340, 2000.

- [40] R. E. Showalter. *Monotone operators in Banach space and nonlinear partial differential equations*, volume 49. American Mathematical Soc., 2013.
- [41] A. Sommerfeld. *Electrodynamics*, translated by eg ramberg, 1952.
- [42] V. Thomée. *Galerkin finite element methods for parabolic problems*, volume 1054. Springer, 1984.
- [43] R. Thompson. The seismic electric effect. *Geophysics*, 1(3):327–335, 1936.
- [44] S. Tyč, L. M. Schwartz, P. N. Sen, and P.-z. Wong. Geometrical models for the high-frequency dielectric properties of brine saturated sandstones. *Journal of applied physics*, 64(5):2575–2582, 1988.
- [45] H. F. Wang. *Theory of linear poroelasticity with applications to geomechanics and hydrogeology*. Princeton University Press, 2017.
- [46] B. S. White. Asymptotic theory of electroseismic prospecting. *SIAM Journal on Applied Mathematics*, 65(4):1443–1462, 2005.
- [47] A. Ženíšek. *Sobolev spaces and their applications in the finite element method*. Vutium Press, 2005.